IEEE Access
Multidisciplinary | Rapid Review | Open Access Journal

Received March 12, 2020, accepted March 18, 2020, date of publication March 23, 2020, date of current version April 7, 2020.

Digital Object Identifier 10.1109/ACCESS.2020.2982412

Coordinated Operation and Planning of Integrated Electricity and Gas Community Energy System With Enhanced Operational Resilience

CHAOXIAN LV[1,4], HAO YU[1], (Member, IEEE), PENG LI[1], (Member, IEEE), KUNPENG ZHAO[2], HAILONG LI[3], AND SHUQUAN LI[2]

[1]Key Laboratory of Smart Grid of Ministry of Education, Tianjin University, Tianjin 300072, China
[2]State Grid Customer Service Centre, Tianjin 300300, China
[3]School of Business, Society and Engineering, Malardalen University, 721 23 Västerås, Sweden
[4]School of Electrical and Power Engineering, China University of Mining and Technology, Xuzhou 221116, China

Corresponding author: Hao Yu (tjuyh@tju.edu.cn)

This work was supported by the National Science Foundation of China under Grant 51961135101 and Grant 51907139.

ABSTRACT The coupling in integrated electricity and gas community energy system (IEGS) provides alternative operation modes when unpredictable outages occur at energy-supply sides. Reasonable operation strategies and system configuration can effectively improve the system's resilience, making reliable and continuous operation feasible. Based on the complementary characteristics and reserve capabilities of IEGS, this paper proposes a multi-stage scheduling strategy for resilience enhancement in which thermal storage serves as emergency response resources. The resilient scheduling framework consists of rolling reserve optimization stage, day-ahead economic dispatch stage and fault restoration stage. With the reserve capacity of energy storage generated by rolling optimization and day-ahead dispatch, multiple forms' critical loads will be satisfied in priority when outage occurs on energy-supply sides. Furthermore, a two-level planning model integrating the resilient operation strategy is formulated to better adapt to the source emergency. The proposed planning method is applied to an IEGS with practical demands as a case study. The results show that the configuration generated by the two-level planning model can satisfy the daily reserve requirements for emergency failures, and the resilient scheduling strategy with storage reserve can improve the system resilience effectively.

INDEX TERMS Integrated electricity and gas community energy system (IEGS), planning, operational resilience, energy storage, energy outage.

NOMENCLATURE

A. ABBREVIATIONS

IEGS	Integrated electricity and gas community energy system
HP	Ground source heat pump
PV	Photovoltaic
WC, DC	Conventional water-cooled chiller, double-duty chiller
IS, IT	Ice-storage system, ice-storage tank
WT, CT, HT	Water tank, cold-water tank, hot-water tank
CWP, HWP	Chilled water pump, heating water pump
EB, EP	Electric boiler, ethylene glycol pump
GT, AC	Gas turbine, absorption chiller

The associate editor coordinating the review of this manuscript and approving it for publication was M. A. Hannan.

B. SETS

$\Omega_{\mathrm{CWP}}^{\mathrm{CT}}$	Set of the CWPs collateral to CTs

C. VARIABLES

$Q_t^{\mathrm{HP,H}}$, $Q_t^{\mathrm{HP,C}}$, $Q_t^{\mathrm{HP,S}}$	Heating, cooling and cooling-storage powers of the HPs at time t (kW)
$U_t^{\mathrm{HP,C}}$, $U_t^{\mathrm{HP,S}}$	Cooling and cooling-storage modes of the HPs at time t
P_t^{HP}, P_t^{WC}	Consumed powers of the HPs and WCs at time t (kW)
P_t^{CT}, P_t^{IS}	Consumed powers of the CTs and IS at time t (kW)
U_t^{CT}, U_t^{HT}	Cooling and heating states of the CTs/HTs at time t

Q_t^{CT}, Q_t^{HT},	Cooling and heating powers of CTs/HTs at time t (kW)
Q_t^{WC}, Q_t^{EB}	Output powers of the WCs and EBs at time t (kW)
$Q_t^{\mathrm{EB,H}}$, $Q_t^{\mathrm{EB,S}}$	Heating and heating-storage powers of the EBs at time t (kW)
Q_t^{IT}, Q_t^{IS}	Cooling powers of the IT and IS at time t (kW)
P_t^{EB}, P_t^{HWP}	Consumed powers of the EBs and HWPs at time t (kW)
$U_{t,i}^{\mathrm{WT,CWP}}$, $U_{t,i}^{\mathrm{IS,CWP}}$	Cooling states of the ith CWP collateral to the WTs and IS at time t
$Q_t^{\mathrm{DC,C}}$, $Q_t^{\mathrm{DC,I}}$	Cooling and ice-making powers of the DCs at time t (kW)
$U_t^{\mathrm{DC,C}}$, $U_t^{\mathrm{DC,I}}$	Cooling and ice-making modes of the DCs at time t
$U_{t,i}^{\mathrm{HWP}}$	Heating state of the ith HWP at time t
W_t^{CT}, W_t^{HT}, W_t^{IT}	Energy stored in the CTs, HTs and IT at time t (kWh)
P_t^{GT}, H_t^{GT}	Electricity and heating powers of the GTs at time t (kW)
Q_t^{AC}, H_t^{AC}	Cooling and absorbed heating powers of the ACs at time t (kW)
P_t^{TL}	Tie-line power at time t (kW)
F_t^{GT}	Consumed gas power of the GTs at time t (kW)
P_t^{PV}	Output power of the PV system at time t (kW)
C_{inv}, C_{ope}	Annual investment cost and annual operation cost (CNY)
M^{IT}	Capacity of the IT (kWh)
M^{PV}	Capacity of the PV system (kW)
N^{HP}, N^{WC}, N^{DC}, N^{EB}	Installed numbers of the HPs, WCs, DCs and EBs
N^{GT}, N^{AC}, N^{WT}	Installed numbers of the GTs, ACs and WTs
N_t^{HP}, N_t^{WC}, N_t^{DC}, N_t^{EB}	Operating numbers of the HPs, WCs, DCs and EBs at time t
N_t^{GT}, N_t^{AC}	Operating numbers of the GTs and ACs at time t

D. PARAMETERS

$\underline{Q}^{\mathrm{HP,C}}$, $\overline{Q}^{\mathrm{HP,C}}$	Lower and upper power limits of the HP for cooling (kW)
$\underline{Q}^{\mathrm{HP,S}}$, $\overline{Q}^{\mathrm{HP,S}}$	Lower and upper power limits of the HP for cooling-storage (kW)
$\underline{Q}^{\mathrm{HP,H}}$, $\overline{Q}^{\mathrm{HP,H}}$	Lower and upper power limits of the HP for heating (kW)
$\overline{W}^{\mathrm{CT}}$, $\overline{W}^{\mathrm{HT}}$	Upper limits of the stored energy in CT and HT (kWh)
$\underline{Q}^{\mathrm{WC}}$, $\overline{Q}^{\mathrm{WC}}$	Lower and upper power limits of the WC (kW)
$\overline{Q}^{\mathrm{IT}}$, $\overline{Q}^{\mathrm{AC}}$	Upper limits of cooling power of the IT and AC (kW)
$\underline{Q}^{\mathrm{DC,C}}$, $\overline{Q}^{\mathrm{DC,C}}$	Lower and upper limits of cooling power of the DC (kW)
$\underline{Q}^{\mathrm{DC,I}}$, $\overline{Q}^{\mathrm{DC,I}}$	Lower and upper limits of ice-making power of the DC (kW)
$\overline{Q}^{\mathrm{HT}}$, $\overline{Q}^{\mathrm{HWP}}$, $\overline{Q}^{\mathrm{EB}}$	Upper power limits of the HT, HWP and EB (kW)
$\overline{Q}^{\mathrm{EP}}$, $\overline{Q}^{\mathrm{IS,CWP}}$	Upper power limits of the EP and CWP collateral to the IS (kW)
$\overline{Q}^{\mathrm{CT,CWP}}$	Upper power limit of the CWP collateral to the CT (kW)
$\overline{P}^{\mathrm{GT}}$	Upper power limit of the GT (kW)
$P^{\mathrm{TL,max}}$, $F^{\mathrm{GT,max}}$	Maximum allowed tie-line power and gas power (kW)
$\varepsilon^{\mathrm{WT}}$, $\varepsilon^{\mathrm{IT}}$	Heat loss rates of the WT and IT
$C_{\mathrm{u}}^{\mathrm{HP}}$, $C_{\mathrm{u}}^{\mathrm{WC}}$, $C_{\mathrm{u}}^{\mathrm{DC}}$, $C_{\mathrm{u}}^{\mathrm{EB}}$	Investment costs per HP, WC, DC and EB (CNY/unit)
$C_{\mathrm{u}}^{\mathrm{GT}}$, $C_{\mathrm{u}}^{\mathrm{AC}}$, $C_{\mathrm{u}}^{\mathrm{WT}}$	Investment costs per GT, AC and WT (CNY/unit)
$C_{\mathrm{c}}^{\mathrm{IT}}$	Investment cost per-unit capacity of IT (CNY/kWh)
$C_{\mathrm{c}}^{\mathrm{PV}}$	Investment cost per-unit capacity of PV (CNY/kW)
C_t^{E}, C_t^{G}	Purchasing prices of electricity and natural gas at time t (CNY/kWh)
$D_{\mathrm{OU}}^{\mathrm{E}}$, $D_{\mathrm{OU}}^{\mathrm{G}}$	Durations of the electricity and gas outages (h)
R^{C}, R^{H}, R^{E}	Percentages of critical cooling, heating and electricity loads

I. INTRODUCTION

Due to the increasing environmental concerns, optimizing the energy structure and building clean and efficient energy systems have become an urgent task for sustainable development [1]. At the meantime, natural gas has been playing an important role in energy consumption because of the merits of cleanliness and high-efficiency [2]. The extensive application of combined heat and power (CHP) and power-to-gas (P2G) units interlinks multiple independent energy systems (i.e., electricity and natural gas) [3] and makes it promising by the multi-energy coupling operation [4]. Integrated electricity and gas community energy system (IEGS), whose energy sources are electricity and natural gas, can utilize the complementary characteristics of electricity and gas [5]; furthermore, it can realize high-efficiency operation through the coordination of energy conversion, storage and consumption [6], and has been widely developed.

The coupling of IEGS can improve the operational flexibility, and the operation objectives such as economic dispatching and accommodation of renewable energy sources (RESs) can be facilitated by regulating multiple controllable energy

conversion and storage devices. Reasonable and effective operation strategies, as well as planning methods, are the keys to achieve these goals. The coupling also brings more risks due to the increased uncertainties, seriously affecting the reliability of system operation. In addition, some extreme emergencies may disturb the system topology or structure and have enormous impact on the continuous operation; thus, the adaptation and response strategies of these risks should be especially focused on.

Many studies on the flexible operation of IEGS have been conducted. Reference [7] adopted the energy hub (EH) model to minimize the energy purchase cost by the coordination of heat pumps, CHP unit and storage devices. And multiple demands including electricity, heating and cooling are well satisfied. A two-stage flexible operation framework for integrated community energy system was proposed in [8], whose first stage is to optimize the power flows and second stage is to make decisions for the Pareto optimality curve. For the hybrid energy system that integrates wind power and multiple storages, a day-ahead scheduling model based on stochastic programming was formulated in [9] to minimize the expected operation cost considering the uncertainties of wind power. In [10], a second-order cone optimization model of gas network was established, and the synergistic operation of integrated electricity-gas system was carried out by alternating direction method of multipliers (ADMM). Considering demand response resources, a robust operation strategy of CHP-based energy system was investigated in [11], and the load uncertainties were considered to ensure the risk-averse operation. In addition to the operation issues, the planning of IEGS is another focus as the type and capacity of the equipment have significant influence on the operation performance. In [12], the capacities of the electric chiller, the CHP unit, as well as the ice-storage system were optimized. The system obtained an improved economic performance by including the storage system. With the variation of supply and demand curves converting to the same quantitative index, ref. [13] developed a novel energy supply and demand matching model to accomplish the economy optimality in the full life cycle. Reference [14] realized the expansion planning of integrated electricity and gas system considering bi-directional conservation between gas-fired devices and P2G units as well as the energy flows in gas and electricity networks. An expansion planning of gas and electricity networks was conducted in [15], and the uncertainties including wind power and load growth were considered by stochastic decentralized approach. Reference [16] introduced a multi-attribute planning method for integrated gas-electricity systems by employing two decision methods, i.e., analytical hierarchy process and weighted sum method.

With the increasing coupling and uncertainties in IEGS, the interdependency analysis of each subsystem to the safety and reliability of whole energy system are indispensable [17]. An integrated analysis model of gas-electricity coupling network was constructed in [18], and the influence of state change in natural gas system on the system performance was explored. In [19], for an integrated energy system with gas and electricity networks, the reliability assessment method was established based on impact-increment, and the impacts of the conversion process between gas and electricity on the reliability were analyzed. On the premise of satisfying loads, the security constraints of gas system were well guaranteed by the coordination of gas and electricity system in [20]. These literatures indicate that the utilization of complementary and regulatory capacities among independent energy subsystems can contribute to a better security and reliability level.

Furthermore, energy disruptions caused by natural disasters or failures also seriously affect the reliable operation, and they are sometimes unpredictable and ineluctable. As an important index to describe the adaptability to uncertain faults and the ability to restore the operation within an acceptable range, operational resilience has been of wide concern [21]. For the power grid resilience, the results of catastrophic experiences were mitigated by using defensive islanding in [22]. Reference [23] discussed the resilient operation of distribution network, and the load curtailment was reduced through the power support of distributed microgrids. Similarly, an interactive framework between the distribution network and microgrids of power-water system was proposed in [24] to improve the resilience against natural disasters. As the coupling between gas and electricity systems, the resilience in IEGS needs to be further investigated. Reference [25] dealt with the random faults of power system by means of demand response strategy, so as to reduce the dependence on gas system. In [26], the defender-attacker-defender formulation was proposed for protecting critical components, which yields a min-max-min problem and was solved by the nested column-and-constraint generation method. In [27], a tri-level robust scheduling model, which comprises preventive stage, worst scenario stage, and corrective stage, was established to adapt to random interruptions of gas and electricity transmission links caused by external faults. Thus, the system resilience was enhanced when facing outages. Treating overhead line vulnerable to fail, ref. [28] studied the coordinated planning of electricity and natural gas transportation systems incorporating resilient operation constraints. Thus, the resilience of power grid was effectively improved. A resilience planning model based on one main problem and two sub-problems was presented in [29] for power-water system with multiple microgrids. Microgrids were utilized as energy sources in the first sub-problem, and emergency generator for water pumps restoration was included as the second sub-problem.

Reserve scheduling can be used as an auxiliary measure to deal with the uncertainties and emergencies of energy supply, which plays an important role in improving the operation resilience [30]. Reference [31] quantified the adjustable margins of CHP unit and established an integrated power and heat dispatching method considering the available reserve capacity of CHP units. The accommodation to the uncertainties of wind power was improved. Reference [32] utilized energy storage of distributed gas storage for contingencies

and presented a robust scheduling method against $N-k$ outages to ensure a reliable operation of power system. An IEGS day-ahead economic dispatch model with regulation reserve and spinning reserve was proposed in [33] to manage the renewable energy uncertainties and $N-1$ contingencies of generators. Considering the failure probability of overhead lines and gas pipelines in IEGS, distributed generators and gas storage were modelled as emergency response resources for enhancing resilience in [34]. Thus, the high-priority gas and electricity loads can be supplied during the outage.

The above literatures mainly focus on the resilience improvement of large-scale system that contains generation and transfer links, by the coordination of alternative supply approaches, utilization of emergency resources as well as the reserve measures. However, facing the failures with complete loss of an energy source on consumer side, how to make full use of the reserve and complementation of different resources to ensure safe and reliable operation is still challenging. Additionally, system configuration has a significant influence on the operational resilience. To obtain a better performance on resilience, the consideration of resilience requirements should be integrated into the planning stage.

In this paper, we propose a coordinated operation and planning method of integrated electricity and gas community energy system with enhanced operational resilience. First, the operation models of electricity-driven and gas-driven devices as well as photovoltaic (PV) system are built. Then, a tri-stage resilient scheduling strategy based on the reserve mode of independent gas and electricity system is proposed, in which the energy storages serve as auxiliary reserve resources for supply-side outages; furthermore, a two-level optimal planning model integrating the resilient scheduling strategy is formulated. Finally, the correctness and effectiveness of the planning model and the resilient scheduling strategy are verified through case studies. The main contributions of this paper are summarized as follows:

1) A multi-stage scheduling strategy with thermal storage reservation is proposed for resilience enhancement. Based on the thermal reserve capacities which are indispensable for critical loads during supply-side outages calculated in rolling stage, day-ahead economic scheduling will be carried out to coordinate the operation of multiple devices with maintaining sufficient reservation. And the fault restoration mode will be adopted to satisfy critical loads by utilizing emergency response characteristics of thermal storages when supply-side outage occurs.

2) Different reserve measures are utilized for unexpected contingencies. Under normal operations, independent gas and electricity systems are treated as the main reserve for each other in case of supply-side outages in addition to economic improvement; moreover, thermal storage devices serve as auxiliary reserve for supporting high-priority loads when the main reserve fails to provide sufficient reserve capacity. Due to little electricity consumption for heating/cooling releasing, thermal storage devices can effectively facilitate the coordinated supply of multiple demands when facing supply-side failures. Thus, a more resilient operation can be achieved with main and auxiliary reserves.

3) A two-level model is established to optimize the system configuration based on the resilient operation strategy. By adopting the genetic algorithm (GA) in the upper level for configuration updating and resilient strategy in the lower level for operation optimization, the configuration maintaining sufficient resilience to emergencies can be obtained.

The rest of this paper is organized as follows. Section II describes the structure and reserve mode of the IEGS. Section III proposes the multi-stage resilient scheduling strategy and the optimal planning model integrated with operational resilience. A two-level solving method is presented in Section IV. Section V selects typical data to conduct the case analysis. Finally, Section VI concludes this paper.

II. SYSTEM STRUCTURE AND RESERVE MODE

For the integrated energy systems with a higher reliability requirement, such as in hospitals and governments, the source outage can bring catastrophic results if normal operation is interrupted. Therefore, it is of significance to develop reasonable planning and scheduling method that can satisfy the resilience demands in actual operation.

The IEGS studied in this paper is considered to provide space cooling in summer, space heating in winter and electricity all year round. A typical IEGS often considers gas turbine (GT) for electricity generation, and the exhaust heat can be recovered to supply space heating by heat exchanger, as well as cooling through absorption chiller (AC). Compared with the higher investment and operation cost of GT, ground source heat pump (HP) is widely chosen as a candidate device for space cooling and heating with the merits of high-efficient and green. And conventional water-cooled chillers (WCs) and electric boilers (EBs) are usually serving as the coordination devices of cooling and heating, respectively. Besides, some renewable energy sources, such as photovoltaic, as well as energy storage devices (electricity storage and thermal storage) can be integrated into the IEGS simultaneously. Cold-water tanks (CTs) and hot-water tanks (HTs) can be equipped for storing cooling and heating energy from HP and EB, and ice-storage system (IS) which is composed of double-duty chillers (DCs) and ice-storage tank (IT) is also extensively adopted due to multiple operation modes. From the perspective of energy-driven form to distinguish, these devices can be divided into electricity-driven and gas-driven. The electricity-driven devices include HP system (HPs and CTs), WC, IS and EB system with accumulator (EBs and HTs); and the gas-driven devices include GT and AC. The combination of GT and AC can be regarded as a combined cooling, heating and power (CCHP) system [12].

A practical multi-energy demand has been presented and satisfied by the system in [35], and the energy consumption of the system is just electricity. But when electricity outage occurs, the system will fail completely. In this paper, a CCHP system (GTs and ACs) is considered to be configured for enhancing the system resilience, as well as for economic

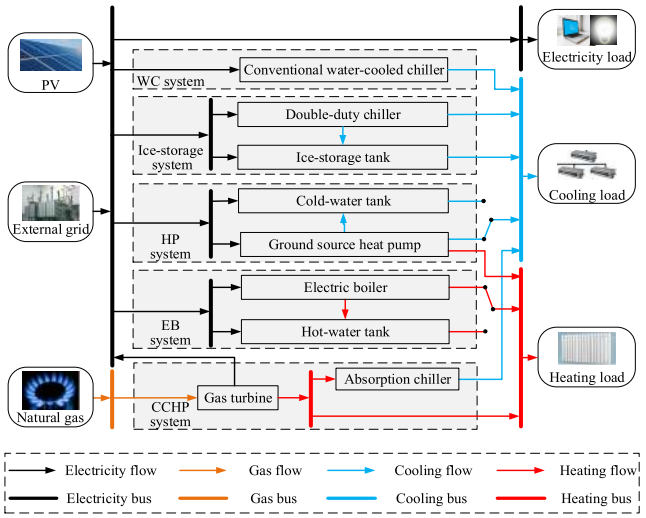

FIGURE 1. Structure and energy flows of the IEGS.

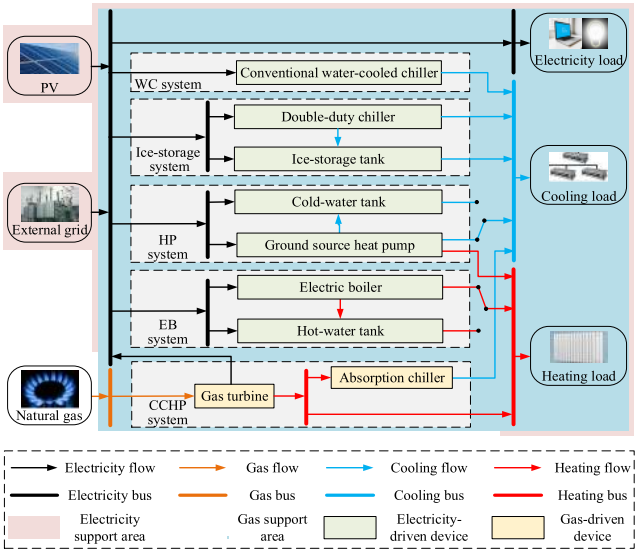

FIGURE 2. Reserve scheme of the gas and electricity subsystems.

improvement. Besides, electrical storages have higher capital costs and limited life cycle, the reserve modes will become extreme complicated; therefore, on the premise of meeting reserve requirements, this paper considers only thermal storages for simplicity. The structure and energy flows of the studied IEGS have been shown in Fig. 1. In cooling season, cooling demand can be satisfied by multiple devices, including ground source heat pump system, conventional water-cooled chillers, ice-storage system, and absorption chillers. In heating season, heating demand may be satisfied by electric boiler system with accumulator, ground source heat pump units or gas turbines. For the electricity demand, it can be met by external power grid, PV and gas turbines. Thus, the above devices consist of the set of main candidate devices whose type and capacity can be further optimized in the following sections. It is necessary to point out that the operation of energy-supply device may require the coordination of auxiliary devices; for example, when the ground source heat pump is in cooling/heating mode, the water pumps on ground source side and load-side need to work simultaneously to carry on energy transfer. And the operation of auxiliary devices requires extra consumption of electrical energy.

The presented IEGS structure in Fig. 1 has two kinds of energy input (electricity and natural gas) and is equipped with electricity-driven and gas-driven devices. Thus, the devices driven by gas and electricity can serve as the reservation for each other. The reserve operating scheme of gas and electricity is shown in Fig.2.

1) When gas supply fails, external grid and RES jointly meet the system electricity load, and the electricity-driven devices and thermal storage devices are coordinated to meet the space cooling/heating demand.

2) In the case of electricity supply failure, gas turbine will be responsible to satisfy the electricity demands of electricity-driven devices, auxiliary devices and electricity load; and the electricity-driven and gas-driven devices work together to meet the cooling or heating demand.

3) Under normal conditions, scheduling strategy should coordinate the operation of electricity-driven and gas-driven devices to improve economic performance according to the load demand and energy purchasing prices.

Therefore, the system presents the characteristics of ''complementation and reserve'' for electricity and gas, which can avoid large-scale loss of critical loads in case that energy supply failure occurs. Note that when the supply of electricity/gas is interrupted, the loads may not be fully satisfied; at this time, reasonable load curtailment should be carried out according to the load importance. In addition, to satisfy the critical loads during gas (electricity) supply failure, the auxiliary reserve of thermal storage devices should be utilized besides the main reserve of the independent electricity (gas) system.

III. OPTIMAL PLANNING MODEL CONSIDERING RESILIENT SCHEDULING STRATEGY

To obtain a design scheme that can satisfy the resilience requirement in actual operation and is able to restore the critical loads when supply-side outage occurs, the optimal planning model incorporating multi-stage resilient scheduling strategy is proposed for system designing and operating. And the operation models of integrated electricity and gas energy system, including the device operation and power balance constraints, are summarized in Appendix.

A. OPTIMAL PLANNING MODEL

1) OBJECTIVE FUNCTION

In this paper, the objective function of IEGS planning is to minimize the overall annual cost, including annual investment cost C_{inv} and annual operation cost C_{ope}:

$$\min F = C_{\text{inv}} + C_{\text{ope}} \tag{1}$$

Annual investment cost:

$$C_{\text{inv}} = \frac{r(1+r)^y}{(1+r)^y - 1} \sum_i C_{\text{inv}}^i \tag{2}$$

where r is discount rate, y is limited lifetime, and C_{inv}^i is initial investment cost of equipment i. The equipment can be divided into two categories: discrete equipment and continuous equipment. The initial investments of discrete equipment and continuous equipment can be calculated by Eq. (3) and Eq. (4), respectively.

$$C_{\text{inv}}^i = C_u^i N^i, \quad i \in \{\text{HP, WC, DC, EB, GT, AC, WT}\} \tag{3}$$
$$C_{\text{inv}}^i = C_{\text{c}}^i M^i, \quad i \in \{IT, PV\} \tag{4}$$

where C_u^i is investment cost per unit of discrete device i and C_{c}^i is investment cost per-unit capacity of continuous device i; N^i and M^i refer to the installed number of discrete device i and the rated capacity of continuous device i, respectively.

Annual operation cost: annual operation cost is the purchasing cost of IEGS. The cost is the sum of energy purchase cost for every day of the base year:

$$C_{\text{ope}} = 365 \sum_{s=1}^{N_{\text{S}}} p_s \sum_{t=1}^{N_{\text{T}}} (C_t^{\text{E}} P_{s,t}^{\text{TL}} + C_t^{\text{G}} F_{s,t}^{\text{GT}}) \Delta t \tag{5}$$

where N_{T} denotes the interval number of a scheduling cycle and N_{S} represents the number of typical scenarios. Moreover, p_s is the probability of scenario s, and $P_{s,t}^{\text{TL}}$ and $F_{s,t}^{\text{GT}}$ are the purchasing electricity power (tie-line power) and gas power at time t in scenario s, respectively.

2) OPTIMAL VARIABLES

The numbers of ground source heat pumps, conventional water-cooled chillers, double-duty chillers, electric boilers, water tanks, gas turbines and absorption chillers, as well as the capacities of ice-storage tank and photovoltaic system, are taken as the optimal variables in this paper, which can be expressed as:

$$X = [N^{\text{HP}}, N^{\text{WC}}, N^{\text{DC}}, N^{\text{EB}}, N^{\text{WT}}, N^{\text{GT}}, N^{\text{AC}}, M^{\text{IT}}, M^{\text{PV}}] \tag{6}$$

In this model, we optimize only the equipped number of water tanks rather than the numbers of cold-water tanks and hot-water tanks, which is in line with the actual planning situation. The water tanks can be used to store the cooling energy in summer and heating energy in winter; thus, the following constraint is added:

$$N^{\text{CT}} = N^{\text{HT}} = N^{\text{WT}} \tag{7}$$

B. MULTI-STAGE RESILIENT SCHEDULING STRATEGY

In actual operation, the supply of electricity and natural gas can be interrupted by an emergency such as natural disaster or system disturbances, and supply-side outages are unpredictable. To ensure the reliable supply of multiple demands, this paper proposes a multi-stage resilient scheduling strategy with the reserve of thermal storage system, including the following stages: 1) rolling optimization of the reserve for supply-side outages; 2) day-ahead economic scheduling with storage reserve; and 3) fault restoration in actual operation.

1) ROLLING OPTIMIZATION STAGE OF THE RESERVE FOR SUPPLY-SIDE OUTAGES

Thermal storage devices can release an amount of cooling/heating by consuming little electricity, and are helpful to break through the limitations of equipment capacities and energy purchasing by reasonable operation strategy. Additionally, the coordination under the fixed operational parameters, such as the heat-electricity ratio of gas turbines, can be balanced by flexible energy storing and releasing of thermal storages. Furthermore, the reliable supply of multiple loads will be enhanced by utilizing the stored energy of thermal storages. When the supply of natural gas or electricity fails, the independent electricity or gas system may not be able to restore the critical loads completely; thus, the reserve of thermal storage becomes a necessary and effective way to achieve the goal of reliable operation.

In this stage, energy management system (EMS) generates the minimum reserve capacity of thermal storage devices that can satisfy the critical loads based on the predicted loads, solar radiation and outage parameters. In each rolling, the objective function is to minimize the initial value of the stored energy of storage systems.

$$\min F_{t_{\text{S}},type} = \sum\nolimits_{i \in \Omega} W_{t_{\text{S}}}^{i,\text{R}} \tag{8}$$

where t_{S} is the beginning interval of the rolling optimization; $type \in \{\text{E, G}\}$, E and G are respectively expressed as electricity outage and gas outage. In the cooling season, $\Omega = \{CT, IT\}$; in the heating season, $\Omega = \{HT\}$. $W_{t_{\text{S}}}^{\text{CT/HT,R}}$ and $W_{t_{\text{S}}}^{\text{IT,R}}$ are the reserve capacities of cold-water/hot-water tank and ice-storage tank, respectively. When electricity outage or gas outage occurs, the tie-line power or gas input is zero, which are shown in Eqs. (9) and (10), respectively. The critical load constraints are depicted in Eqs. (11)-(13).

$$P_t^{\text{TL}} = 0, \quad t = t_{\text{S}}, t_{\text{S}}+1, \ldots, t_{\text{S}} + D_{\text{OU}}^{\text{E}} - 1, \text{ if electricity outage occurs} \tag{9}$$
$$F_t^{\text{GT}} = 0, \quad t = t_{\text{S}}, t_{\text{S}}+1, \ldots, t_{\text{S}} + D_{\text{OU}}^{\text{G}} - 1, \text{ if gas outage occurs} \tag{10}$$
$$Q_t^{\text{HP,C}} + Q_t^{\text{CT}} + Q_t^{\text{WC}} + Q_t^{\text{IS}} + Q_t^{\text{AC}} \geq R^{\text{C}} L_t^{\text{C}} \tag{11}$$
$$Q_t^{\text{HP,H}} + Q_t^{\text{EB,H}} + Q_t^{\text{HT}} + H^{\text{GT}} \geq R^{\text{H}} L_t^{\text{H}} \tag{12}$$
$$P_t^{\text{TL}} + P_t^{\text{PV}} + P_t^{\text{GT}} - (P_t^{\text{HP}} + P_t^{\text{CT}} + P_t^{\text{WC}} + P_t^{\text{IS}} + P_t^{\text{EB}} + P_t^{\text{HWP}}) \geq R^{\text{E}} L_t^{\text{E}} \tag{13}$$

where D_{OU}^{E} and D_{OU}^{G} are the duration of electricity outage and gas outage, R^{C}, R^{H} and R^{E} are the percentages of critical cooling, heating and electricity loads, respectively; and L_t^{C}, L_t^{H}, and L_t^{E} are cooling, heating and electricity loads at time t, respectively.

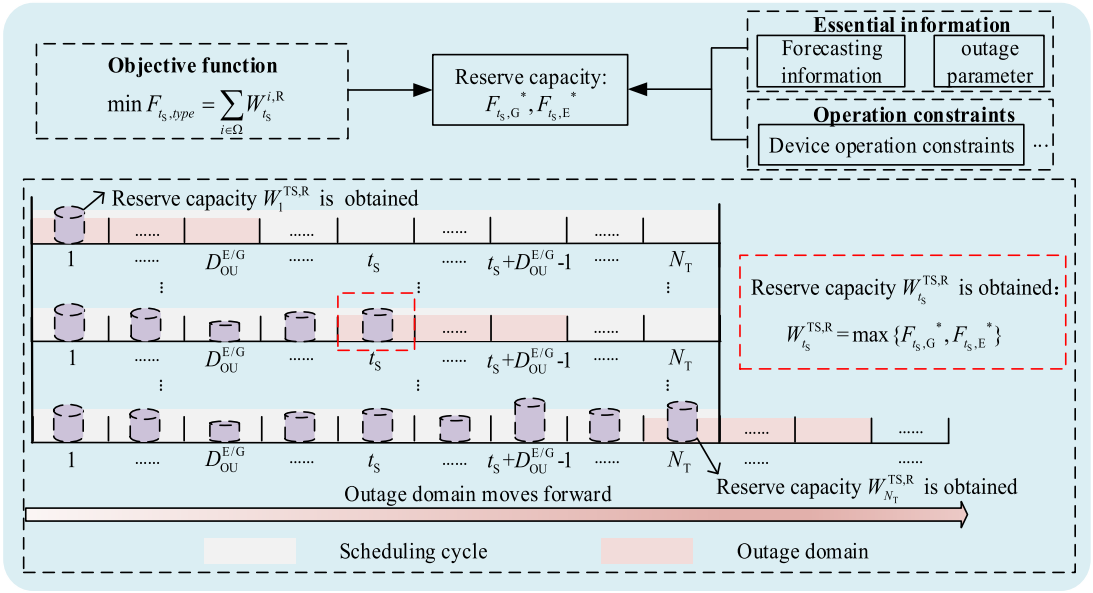

FIGURE 3. Schematic of the rolling optimization for reserve.

The compact form model of rolling stage can be written as:

$$\begin{cases} \min F_{t_S,type} \\ \text{s.t. (A.1)} - \text{(A.54)}, \text{(A.58)} - \text{(A.59)}, \\ \quad (9)/(10), (11) - (13) \end{cases} \tag{14}$$

where the constraints include the operational constraints of devices, (A.1)-(A.54); the power constraints of purchasing electricity and gas, (A.58)-(A.59); the outage constraints, (9)/(10); and the supply constraints of critical loads, (11)-(13).

Therefore, the final reserve capacity $W_{t_S}^{\mathrm{TS,R}}$ at t_S considering multiple outages can be calculated with the following equation:

$$W_{t_S}^{\mathrm{TS,R}} = \max\{F_{t_S,\mathrm{E}}^{*}, F_{t_S,\mathrm{G}}^{*}\} \tag{15}$$

where $F_{t_S,\mathrm{E}}^{*}$ and $F_{t_S,\mathrm{G}}^{*}$ are the reserve capacities for electricity outage and gas outage at time t_S, respectively. The maximal capacity can guarantee that the system has enough reserve for various types of energy outages.

The schematic of rolling optimization for the reserve is shown in Fig. 3. At t_S, the thermal reserve capacity $W_{t_S}^{\mathrm{TS,R}}$ is obtained by the optimization solution based on the outage domain, i.e., t_S to $t_S+D_{\mathrm{OU}}^{\mathrm{E/G}}-1$. With the outage domain continuously moving forward, this rolling process repeats until the reserve calculation is finished for all scheduling intervals.

2) DAY-AHEAD ECONOMIC SCHEDULING STAGE WITH STORAGE RESERVE

After obtaining the reserve capacity of thermal storage device, day-ahead economic scheduling considering the constraints of energy storage reserve capacity is carried out. EMS generates the multi-period scheduling plan for execution based on the forecasting information of solar radiation, multiple energy demands and the generated reserve capacity. The scheduling plan shows the on/off state, operation condition, power of the energy supply and storage equipment.

The objective function is to minimize the overall operation cost in a scheduling cycle, including the purchase cost of electricity and natural gas:

$$\min F_2 = \sum\nolimits_{t=1}^{N_{\mathrm{T}}} (C_t^{\mathrm{E}} P_t^{\mathrm{TL}} + C_t^{\mathrm{G}} F_t^{\mathrm{GT}}) \Delta t \tag{16}$$

where Δt represents the scheduling interval. At the same time, the scheduling should fully consider the constraints of energy storage reserve, as well as the terminal energy restriction of thermal storage devices. Thus, the following operating constraints on thermal storage should be added:

$$W_t^{\mathrm{TS}} = \sum\nolimits_{i\in\Omega} W_t^i \geq W_{t+1}^{\mathrm{TS,R}}, \quad t = 1, 2, \ldots, N_{\mathrm{T}}-1 \tag{17}$$

$$\sum\nolimits_{i\in\Omega} W_t^i \geq W_{1,\mathrm{F}}^{\mathrm{TS,R}}, \quad t = N_{\mathrm{T}} \tag{18}$$

Eq. (17) indicates that the stored energy of the thermal storage devices at time t should meet the reserve demand for different outages at time $t+1$. Meanwhile, the reserves of thermal storage devices make the coupling of different scheduling cycles tighter, and the relationship between the terminal energy and the reserve of adjacent period for thermal storage devices is shown in Eq. (18). Where the subscript F denotes the parameter related to the next scheduling cycle. The schematic of day-ahead economic scheduling with reserve of thermal storage is shown in Fig. 4.

The compact form of the day-ahead economic scheduling with storage reserve can be written as:

$$\begin{cases} \min F_2 \\ \text{s.t. (A.1)} - \text{(A.59)}, (17) - (18) \end{cases} \tag{19}$$

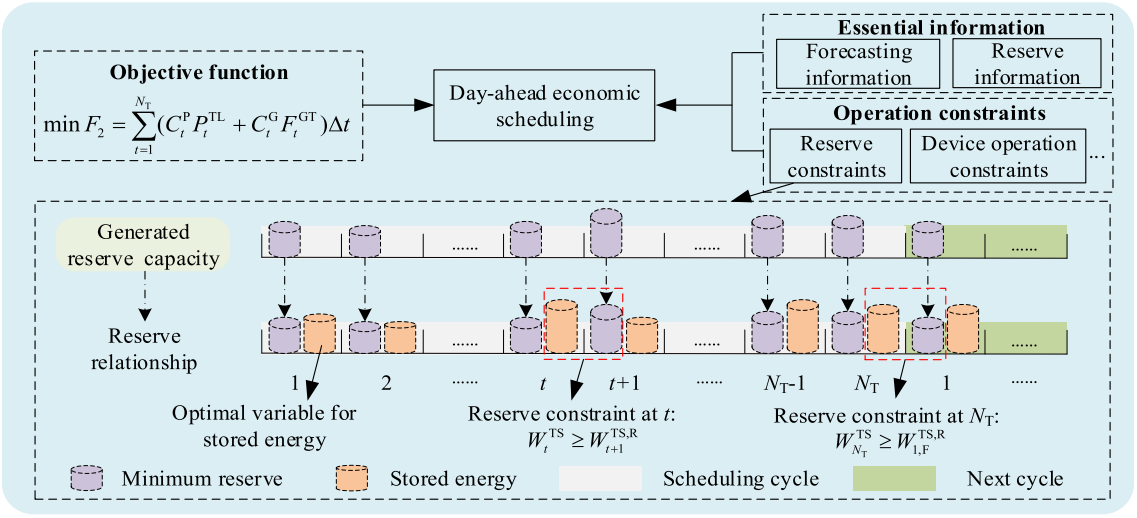

FIGURE 4. Schematic of day-ahead economic scheduling with reserve of thermal storage.

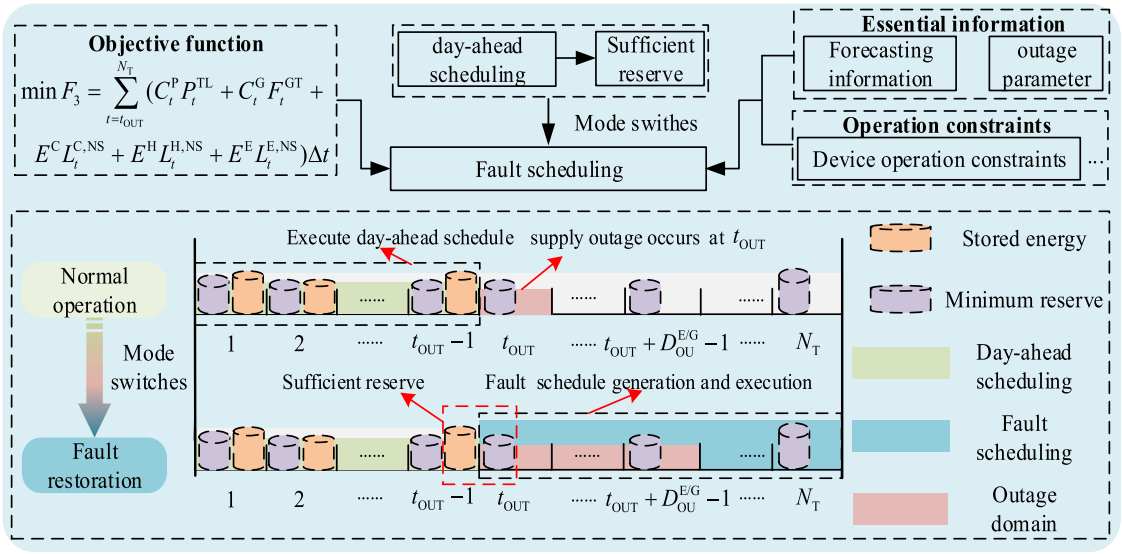

FIGURE 5. Switching and operation process of the fault restoration mode.

where the constraints include the operational constraints of devices, (A.1)-(A.54); the power balance constraints, (A.55)-(A.57); the power constraints of purchasing electricity and gas, (A.58)-(A.59); and the reserve constraints, (17)-(18).

3) FAULT RESTORATION STAGE IN ACTUAL OPERATION

In the process of executing the day-ahead schedule, energy management system will switch to fault restoration mode when the failure of energy supply occurs. The scheduling of remaining time will be generated to satisfy the critical loads of outage period and the full loads of following normal periods. It should be noted that fault restoration scheduling will contain only the outage intervals of the scheduling cycle and the adjacent scheduling cycle if the outage domain spans two scheduling cycles. Fig. 5 shows the mode switching and operation process.

The objective function of fault restoration in the remaining period (the outage time to the end of the scheduling cycle) is to minimize the operation cost and the load curtailment cost:

$$\min F_3 = \sum_{t=t_{OUT}}^{N_T}(C_t^E P_t^{TL} + C_t^G F_t^{GT} + E^C L_t^{C,NS} + E^H L_t^{H,NS} + E^E L_t^{E,NS})\Delta t \quad (20)$$

where t_{OUT} is the beginning time of the outage; $L_t^{C,NS}$, $L_t^{H,NS}$ and $L_t^{E,NS}$ are the curtailed cooling, heating and electricity loads at time t; similarly, E^C, E^H and E^E denote the corresponding punishment costs of curtailed unit loads.

When electricity/gas outage occurs, the tie-line power or gas injection during the period is zero, which can be described

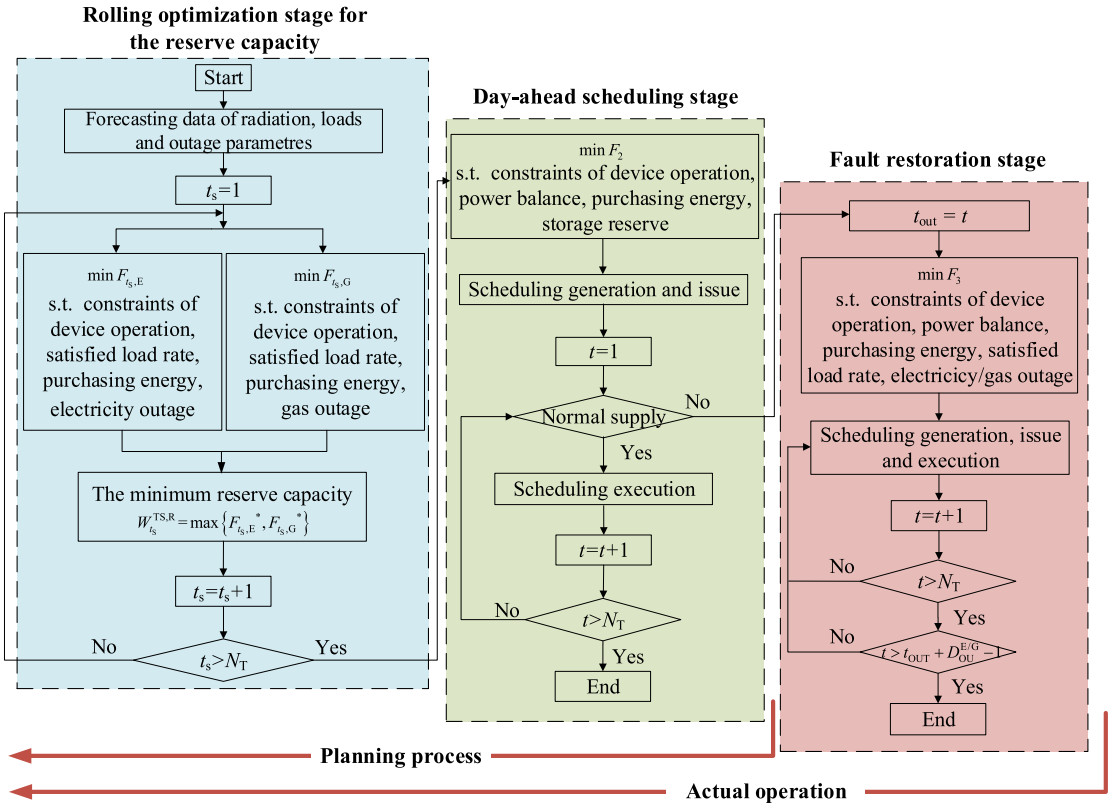

FIGURE 6. Resilience scheduling strategy of IEGS with storage reserve.

as follows:

$$P_t^{TL}=0,\quad t=t_{OUT},t_{OUT}+1,\ldots,t_{OUT}+D_{OU}^{E}-1,\quad \text{if electricity outage occurs} \tag{21}$$

$$F_t^{GT}=0,\quad t=t_{OUT},t_{OUT}+1,\ldots,t_{OUT}+D_{OU}^{G}-1,\quad \text{if gas outage occurs} \tag{22}$$

Eqs. (23)-(25) are the power balance constraints of cooling, heating, and electricity in fault restoration mode. To prevent large load curtailments when adjusting supply ratios to minimize the objective and ensure that the critical loads can be fully satisfied, constraints (26)-(28) are added. It should be noted that load curtailment can be reduced, even avoided, by setting reasonable penalty costs for curtailed loads when adopting the restoration strategy in post-fault period of fault mode.

$$Q_t^{HP,C}+Q_t^{CT}+Q_t^{WC}+Q_t^{IS}+Q_t^{AC}=L_t^{C}-L_t^{C,NS} \tag{23}$$

$$Q_t^{HP,H}+Q_t^{EB,H}+Q_t^{HT}+H^{GT}=L_t^{H}-L_t^{H,NS} \tag{24}$$

$$P_t^{TL}+P_t^{PV}+P_t^{GT}=L_t^{E}+P_t^{HP}+P_t^{CT}+P_t^{WC}+P_t^{IS}+P_t^{EB}+P_t^{HWP}-L_t^{E,NS} \tag{25}$$

$$L_t^{C,NS}\le(1-R^{C})L_t^{C} \tag{26}$$

$$L_t^{H,NS}\le(1-R^{H})L_t^{H} \tag{27}$$

$$L_t^{E,NS}\le(1-R^{E})L_t^{E} \tag{28}$$

The compact model of outage mode operation can be written as:

$$\begin{cases}\min\ F_3\\ \text{s.t. (A.1)}-\text{(A.54)}\,,\ \text{(A.58)}-\text{(A.59)}\,,\\ \quad\text{(21)}\,/\text{(22)},\ \text{(23)}-\text{(28)}\end{cases} \tag{29}$$

where the constraints include device operational constraints, (A.1)-(A.54); the power constraints of purchasing electricity and gas, (A.58)-(A.59); the outage constraints, (21)/(22); the power balance constraints, (23)-(25); and the supply constraints of critical loads, (26)-(28).

In practice, the application and coordination of the proposed scheduling strategy are depicted in Fig. 6. Based on the state and forecasting data of IEGS, the minimum reserve capacity of thermal storage for source emergency are generated by the rolling stage. Then, the day-ahead schedule is generated and delivered to the devices for execution with the constraints of storage reserve and system operation. At each interval, the corresponding orders, which contain the ON/OFF state of each unit, the operation condition, and the corresponding power of each subsystem, will be delivered to the local control system for execution. In case of source-side failure, the system will switch to fault restoration mode from day-ahead scheduling to satisfy the critical loads in priority. The scheduling ends when the executions of all intervals' schedules in a scheduling day, as well as the outage domain, are completed. The proposed framework provides a novel resilient operation of IEGS by a multi-stage scheduling

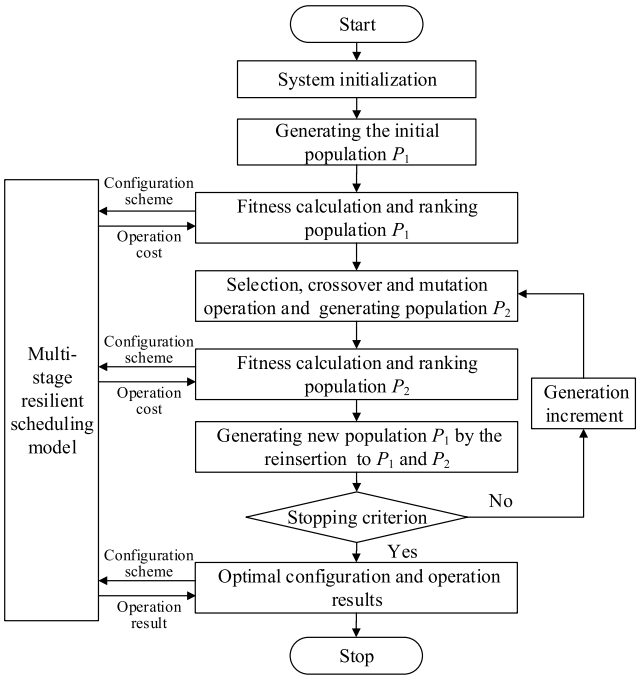

FIGURE 7. Flow chart of the two-level solving method.

strategy. Based on rolling reservation, economic scheduling and fault restoration, the strategy regulates multiple flexible links to facilitate the system resilience, as well as economic performance.

IV. SOLVING OF THE IEGS PLANNING

The formulated optimization problem contains plenty of integer variables and continuous variables, which brings significant challenges to the problem solving. Thus, a two-level solving framework is adopted to decouple the planning and operation problems, where the upper level is to optimize the system configuration and the lower level is to simulate the resilient operation strategy. Meanwhile, the typical operation scenarios can also be calculated in parallel. Thus, the calculation complexity of the problem can be further decreased. Through the interaction between the upper and lower levels, the configuration with sufficient resilience in actual operation will be obtained. Genetic algorithm is used for solving the optimization problem of upper level due to its high efficiency, parallelism and global searching [36]. After linearizing the nonlinear items by the method in [35], the optimization of lower level is transferred to a mixed-integer linear programming (MILP) problem and is solved by ILOG's CPLEX 12.8 solver [37]. The flow chart based on the genetic algorithm is shown in Fig. 7. The detailed solving procedure is illustrated as follows:

1) System initialization. The system structure, operation and investment parameters of candidate devices, load profiles and energy prices will be used to initialize the algorithm. Besides, the parameters of genetic algorithm, including the maximum evolutionary generation, selection, crossover, mutation and reinsertion rates, will also be read.

2) Population initialization. A random set of N individuals is generated, which will act as the initial population P_1. Each individual of the population is a set of the configuration variables, i.e., the numbers of ground source heat pumps, conventional water-cooled chillers, double-duty chillers, electric boilers, water tanks, gas turbines and absorption chillers and the capacities of ice-storage tank and photovoltaic system, as shown in Eq. (6).

3) Fitness calculation of the population P_1 and ranking the population. Here, the configuration variables of each individual in P_1 will be delivered to the operation model as a configuration scheme; and the multi-stage resilient scheduling strategy is called to calculate the operation performance of each typical scenario for each individual. The decision variables during scheduling contain the ON/OFF state of each unit, operating mode and power of each subsystem. Thus, annual operation cost and overall annual cost for each individual can be obtained by Eq. (5) and Eq. (1), respectively. Then, the fitness value of each individual will be evaluated by the ranking of the overall cost for all individuals.

4) Selection, crossover, and mutation. Select the best-ranking individuals from population P_1 to reproduce new population according to the selection rate, and breed new individuals through crossover and mutation operations at certain probabilities (crossover and mutation rates). Thus, population P_1 is updated and the offspring P_2 will be generated.

5) Fitness calculation and ranking the population P_2. Similar to Step 3), the fitness of all individuals for population P_2 will be calculated and ranked.

6) Generating a new population. To maintain the size of the original population, an updated population P_1 with N individuals will be obtained by the reinsertion of P_2 into P_1 based on the individual fitness. The reinsertion rate indicates the percentage of the offspring P_2 that will be chosen to insert to P_1. Thus, N individuals with larger fitness values will be selected from population $\{P_1 \cup P_2\}$ to the next generation.

7) Stopping criterion. If the maximum evolution generation has been reached, the evolution terminates and the optimal configuration, as well as the operation status of each typical scenario, will be determined; otherwise, it returns to Step 4) for next-generation evolution.

Note that the process of calling the resilient scheduling model (operation level) for the fitness calculation comprises only the first two stages, i.e., the rolling optimization stage for reserve and the day-ahead scheduling stage with storage reservation; and the operation cost will be delivered to the configuration level for the fitness calculation. The last stage (fault restoration stage) is to guarantee the supply of the critical loads in the event of supply-side outages in actual operation based on the reserves and operation conditions of the first two stages.

In actual planning process, the essential information, such as the typical load profile, set and parameters of candidate devices and so on, should be input firstly after the analysis of

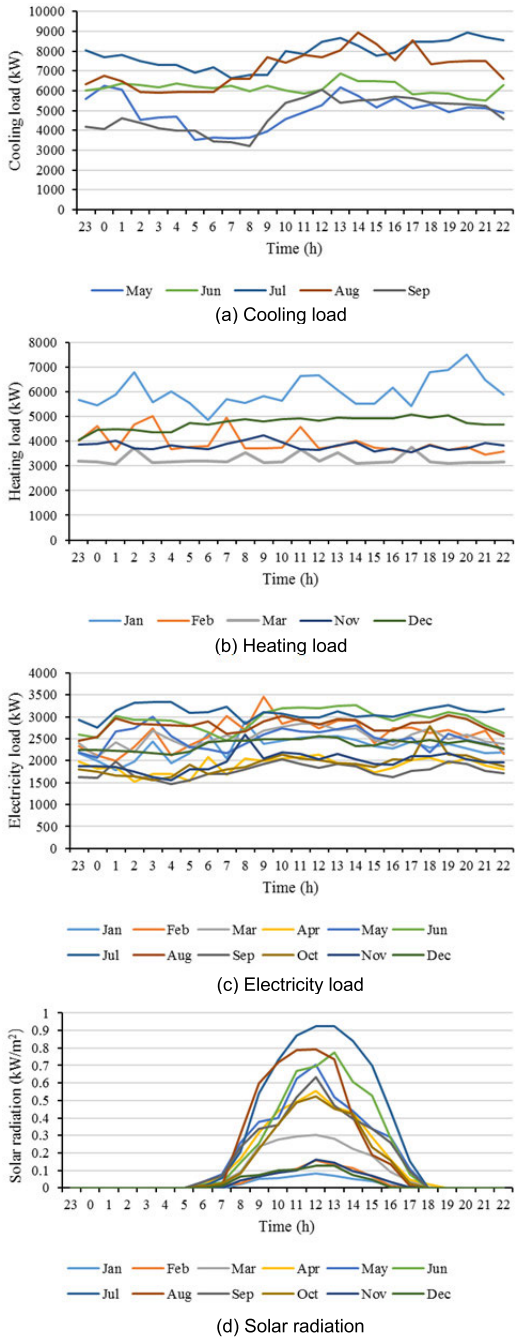

FIGURE 8. Loads and solar radiation of the typical scenarios (Jan-Dec correspond to Scenarios 1-12).

system demand characteristics. Then, the solving algorithm can run automatically through the interaction between GA algorithm of the upper level and resilient strategy of the lower level. And the configuration considering the resilience demand in actual operation will be obtained. The proposed framework provides a practical planning method for getting a balance between economic performance and resilient operation, and is meaningful to achieve the coordinated operation and planning for community system with enhanced resilience, especially for the system with a higher reliability requirement.

TABLE 1. Candidate equipment parameters for operation and investment [12], [38].

Item		Rated capacity (per unit)	Coefficient of performance/ efficiency	Investment cost /$\times 10^4$ CNY
Discrete equipment	HP	Cooling-1162 kW /Heating-1355 kW	Cooling-5.38 /Heating-4.14	300/unit
	WC	3164 kW	5.13	350/unit
	DC	Cooling-3164 kW /ice-making-2341 kW	Cooling-4.89 /ice-making-4.03	400/unit
	WT	Cooling storage-10000 kWh /Heating storage-22000 kWh	---	100/unit
Continuous equipment	EB	2050 kW	0.99	150/unit
	GT	1200 kW	Electricity-0.35 /heat-0.4	0.68/kW
	AC	800 kW	1.2	0.12/kW
	IT	---	---	0.007/kW
	PV	---	---	0.75/kW

V. CASE STUDY

This section applies the two-level planning model described above to a community energy system with practical demands in north China. The cooling/heating demands of the system have seasonal characteristics: space cooling and electricity are needed in cooling period (May to September), space heating and electricity are needed in heating period (November to March), and only electricity is needed in the mid-period (April and October).

The operation data of typical scenarios during the cooling and heating periods, as well as mid-period, are selected as the basic data for system planning. According to the seasonal and hourly variations of loads and solar radiation, one typical scenario is introduced to represent the operation of each month; thus twelve typical scenarios can be obtained, as shown in Fig. 8. And the probability of each typical scenario is 1/12. As seen from the figure, there are significant differences between these scenarios: the load compositions are different in different supply periods; during the same supply period, the overall load levels, variation trends and peak values also differ significantly. Additionally, the overall cooling and heating demand levels are strongly correlated with the solar radiation, and the higher radiation corresponds to higher cooling demand and lower heating demand.

The operation and investment parameters of candidate devices are listed in Table. 1. The detailed performance

TABLE 2. Electricity and natural gas purchasing tariffs.

Item	Maximum power	Category	Period	Price/(CNY/kWh)
Electricity	10MW	Peak	8:00-11:00, 18:00-23:00	1.35
		Valley	00:00-7:00, 23:00-00:00	0.47
		Flat	7:00-8:00, 11:00-18:00	0.89
Natural gas	5MW	---	Whole day	0.4

parameters of the devices and their auxiliary devices can refer [35]. The time of use (TOU) tariff of electricity and the purchasing tariff of natural gas in the IEGS are presented in Table 2. The maximum cooling and heating powers of water tank are 1322 kW and 2933 kW, respectively. The maximum power of ice-storage tank is 7000 kW.

The scheduling period is from 23:00 to 22:00 the next day, and the scheduling interval is one hour, i.e., a whole scheduling cycle contains 24 scheduling intervals. Due to the restriction of roof area, the maximum capacity of the PV system is 1000 kWp. The critical percentages of the cooling, heating and electricity loads are 80%, 80% and 70%, respectively; similarly, penalty costs of the curtailed cooling, heating and electricity loads are 60 CNY/kWh, 60 CNY/kWh and 100 CNY/kWh, respectively, [39]. The outage durations of the electricity and natural gas supply are 2 hours and 4 hours. A life cycle of 20 years for all devices and a discount rate of 0.08 are assumed for the system. For the genetic algorithm, the individual size of one population is 30, the maximum evolutionary generation is 100, the selection, crossover and mutation rates are 0.7, 0.8 and 0.3, and the reinsertion rate is 0.6.

To verify the correctness and effectiveness of proposed planning method and resilient scheduling strategy, the analysis of planning and operation results with resilient scheduling strategy and the comparison with the traditional method are conducted. And the traditional method refers to the planning without considering resilient scheduling strategy [40].

A. ANALYSIS OF THE PLANNING AND OPERATION RESULTS WITH THE RESILIENT SCHEDULING STRATEGY

1) PLANNING RESULTS OF THE RESILIENT SCHEDULING STRATEGY

Based on the typical operation scenarios and the resilient scheduling strategy, the optimal configuration of the IEGS is obtained, as summarized in Table 3.

Table 3 shows that the system is equipped with both electricity-driven devices and gas-driven devices to take full advantage of the superiority of complementation and reservation of gas and electricity subsystems for reliability and economy. And the capacity of PV reaches the upper limit to provide electricity using solar energy. Furthermore, the system is equipped with multi-type thermal storage devices,

TABLE 3. Optimal configuration incorporating the resilient scheduling.

Category	Configuration	Investment cost /$\times 10^4$ CNY	Annual cost /$\times 10^4$ CNY
Overall annual cost	---	---	2821.7
Annual investment cost	---	---	575.3
Annual operation cost	---	---	2246.4
Ground source heat pump	3	900.0	---
Conventional water-cooled chiller	1	350.0	---
Double-duty chiller	1	400.0	---
Ice-storage tank	10009.0 kWh	70.1	---
Electric boiler	1	150.0	---
Water tank	1	100.0	---
Gas turbine	3	2448.0	---
Absorption chiller	5	480.0	---
Photovoltaic	1000 kW	750	---

including one ice-storage tank and one water tank; the operation economy can be improved through energy storage/release under the TOU tariff mechanism, as well as the adaptation to source emergency. Meanwhile, ground source heat pump has a higher COP and can work in cooling/cooling-storage mode in summer and heating mode in winter; thus the system is configured with several heat pumps. In order to play the role of ice-storage tank and water storage tank, a double-duty chiller and an electric boiler are also installed. In addition, the introduction of conventional water-cooled chiller can promote the complementation and coordination of energy supply/storage devices for economic improvement. And the above configuration was obtained by minimizing the overall annual cost to maintain a balance between economy and resilience; with the constraints of multi-stage resilient strategy, the configuration is with abundant energy conversion devices and reserve capacity to cope with the source emergency in actual operation.

2) RESULTS OF THE DAY-AHEAD SCHEDULING CONSIDERING RESILIENT SCHEDULING STRATEG

a: COOLING PERIOD

Scenario 7 (July) with a high load level was selected to analyze day-ahead operation during the cooling period. Fig. 9 presents the power balance of Scenario 7. As can be seen from the figure, at night (23:00-07:00), most of the cooling loads are satisfied by electricity-driven chillers, and the electricity loads are mainly satisfied by external power grid, as the electricity price is cheaper. In other periods, the price of natural gas is relatively low, and the gas turbines burn natural gas to supply electric power while the chiller absorbs waste heat for refrigeration. The insufficiency of cooling and electricity

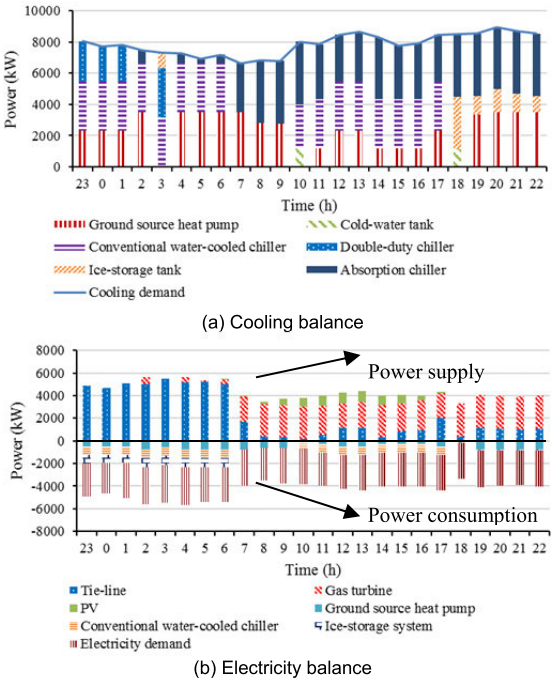

FIGURE 9. Power balance in the cooling period.

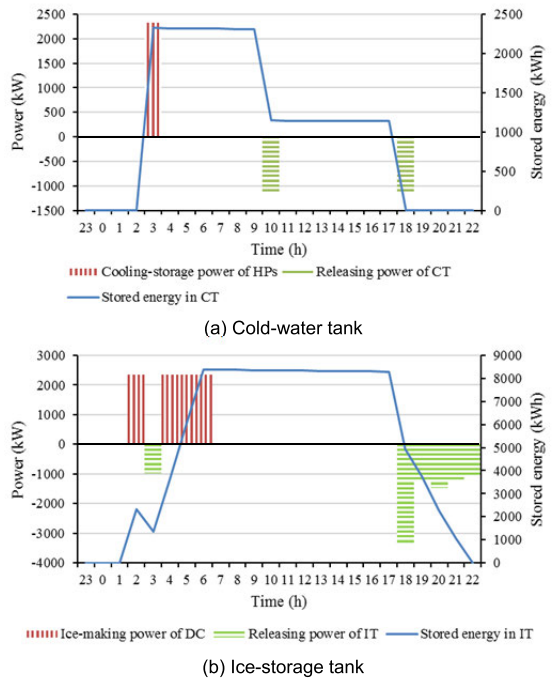

FIGURE 10. Stored energy of the thermal storage devices in the cooling period.

demands will be covered by electricity-driven devices and external grid respectively. The proposed scheduling considers the TOU price and the price difference between electricity and gas, and coordinates the operation of electricity-driven and gas-driven devices to achieve a better economy.

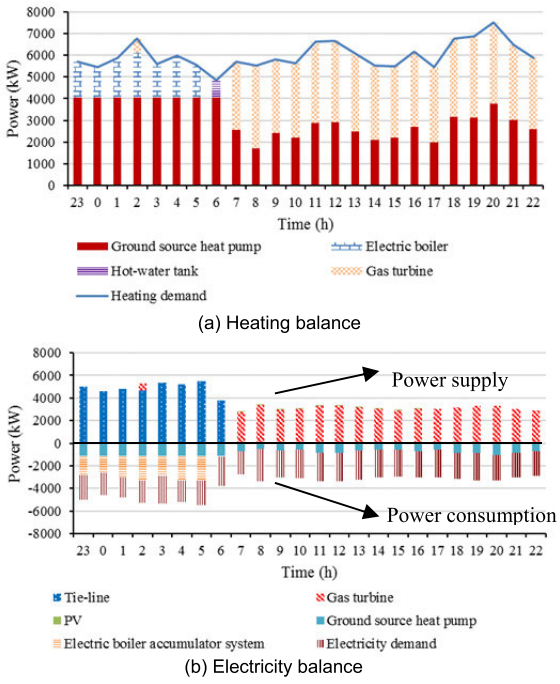

FIGURE 11. Power balance in the heating period.

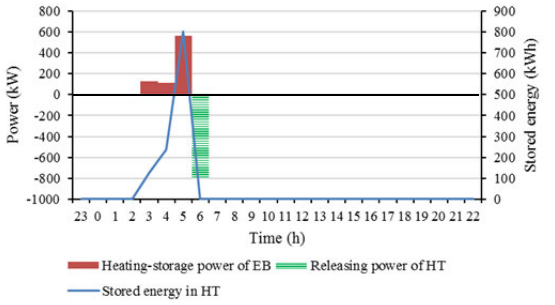

FIGURE 12. Stored energy of the hot-water tank in the heating period.

The curves of thermal storage devices are depicted in Fig. 10. To utilize the energy storage devices for economic improvement, the characteristics of ''valley to charge and non-valley to discharge'' are expected. But with the constraints of resilience reserve and power balance, the charge-discharge behaviors need to be adjusted according to practical situations. Thus, energy storage takes place in the valley period with energy releasing mostly in the flat-peak period. In 3:00-4:00, as the heat pumps are in cooling-storage mode and incompatible with cooling mode, the ice-storage tank releases energy to compensate cooling vacancy as well as for economic needs.

b: HEATING PERIOD

Similarly, Scenario 1 (January) with higher heating load was analysed as an example of the heating period. The power balance and stored energy of hot water tank are shown in Fig. 11 and Fig. 12, respectively. Similar to the cooling

TABLE 4. Reserve capacity and stored energy in Scenario 7 of cooling period.

Time	23	0	1	2	3	4
Stored energy	0	0	0	2341.0	3691.5	6028.8
RC	0	0	0	0	0	0
Time	5	6	7	8	9	10
Stored energy	8363.8	10696.4	10685.8	10675.1	10664.4	9491.7
RC	0	0	0	0	0	0
Time	11	12	13	14	15	16
Stored energy	9482.2	9472.8	9463.3	9453.8	9444.4	9343.9
RC	0	0	0	0	0	0
Time	17	18	19	20	21	22
Stored energy	9425.5	4929.6	3740.3	2266.7	1052.0	0
RC	366.8	366.4	0	0	0	0

(RC-reserve capacity of thermal storage)

TABLE 5. Reserve capacity and stored energy in Scenario 1of heating period.

Time	23	0	1	2	3	4
Stored energy	0	0	0	0	126.0	238.9
RC	0	0	0	0	0	0
Time	5	6	7	8	9	10
Stored energy	802.1	0	0	0	0	0
RC	0	0	0	0	0	0
Time	11	12	13	14	15	16
Stored energy	0	0	0	0	0	0
RC	0	0	0	0	0	0
Time	17	18	19	20	21	22
Stored energy	0	0	0	0	0	0
RC	0	0	0	0	0	0

(RC-reserve capacity of thermal storage)

period, the electricity and natural gas are the main suppliers of the valley period and non-valley period, respectively. The electric boiler system mainly plays the role of energy regulation on account of its lower efficiency: at 3:00-6:00, the electric boiler participates in supplying heating with the heat pumps and storing heating to the hot-water tank, and the stored energy is released for heating at 6:00-7:00, as shown in Fig. 12.

3) RESERVE CAPACITY OF THE THERMAL STORAGE DEVICES

The reserve capacity of the thermal storage devices in Scenario 7 (July) of the cooling period is presented in Table 4. To ensure the supply of critical loads, the thermal storage devices need to maintain reserve energy to enhance the ability for the supply-side outage, especially in the intervals which have higher loads. At the same time, the total stored energy of ice storage tank and cold-water tank in the day-ahead scheduling plan is larger than the required reserve capacity; thus, the system maintains enough resilience for utilizing the reserve characteristics to handle supply-side outages and satisfy the critical loads. In the heating period, because of the adequate equipment capacity and relatively lower heating load compared with the cooling period, the independent gas/electricity subsystem which acts as the main reserve can meet the critical loads by itself if the electricity/natural gas supply is interrupted. Therefore, thermal storage devices are not required to maintain reserve energy, as shown in Table 5.

B. COMPARISON OF THE PLANNING AND OPERATION WITH AND WITHOUT THE RESILIENT STRATEGY

This subsection mainly compares and analyses the configuration, reserve state and fault restoration ability with and without considering the resilient strategy.

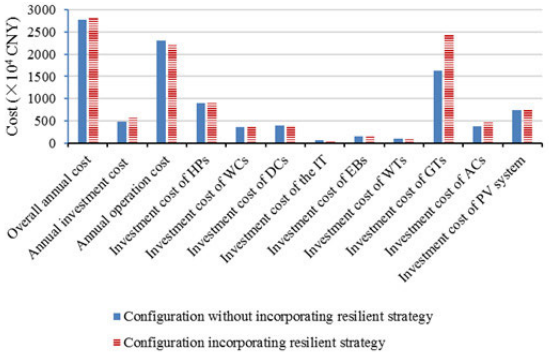

FIGURE 13. Configuration comparisons incorporating resilience strategy or not.

1) PERFORMANCE COMPARISON OF THE CONFIGURATION WITH AND WITHOUT THE RESILIENT STRATEGY

The configuration without considering the resilience strategy is listed in Table 6. The configurations incorporating the resilient strategy or not are compared in Fig. 13. After considering the operation resilience, the system needs to be equipped with more flexible and controllable resources to meet the critical loads in case of source failure, as well as the reserve requirements in normal operation; hence, more gas turbines and absorption chillers, larger capacity of the ice storage tank are optimized. Although the reserves of thermal storage devices may restrict the improvement in the economy, the annual operation cost after considering the resilient strategy is 553,000 CNY lower than before due to the increase of dispatching resources, which are 22,464,000 CNY and 23,017,000 CNY, respectively. The overall annual cost with the resilient strategy is 381,000 CNY (1.4%) higher than that without the resilient strategy; the proposed planning method can realize reliability improvement at a small economic cost.

TABLE 6. Optimal configuration without considering resilient scheduling.

Category	Configuration	Investment cost /$\times 10^4$ CNY	Annual cost /$\times 10^4$ CNY
Overall annual cost	---	---	2783.6
Annual investment cost	---	---	481.9
Annual operation cost	---	---	2301.7
Ground source heat pump	3	900	---
Conventional water-cooled chiller	1	350	---
Double-duty chiller	1	400	---
Ice-storage tank	9337.0 kWh	65.4	---
Electric boiler	1	150	---
Water tank	1	100	---
Gas turbine	2	1632	---
Absorption chiller	4	384	---
Photovoltaic	1000 kW	750	---

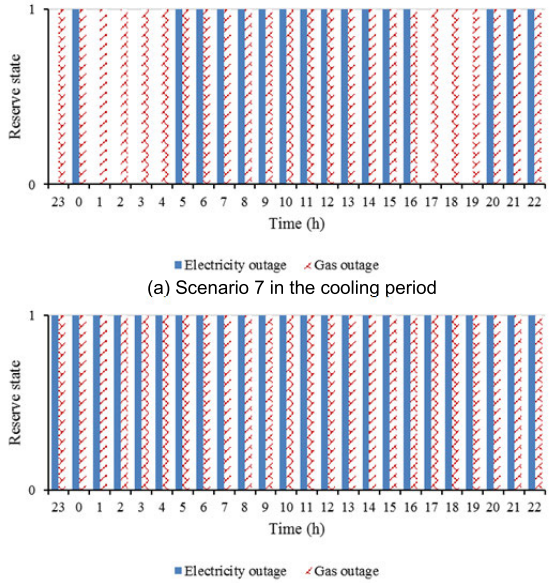

(a) Scenario 7 in the cooling period

(b) Scenario 1 in the heating period

FIGURE 14. Reserve states under the configuration without incorporating resilience strategy.

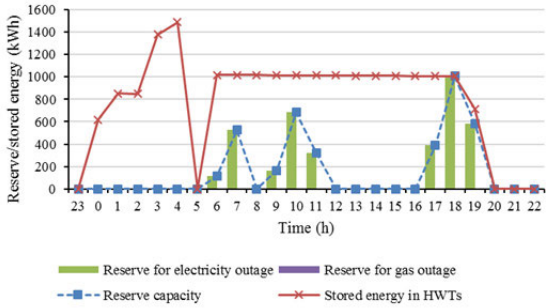

FIGURE 15. Storage reserve under the configuration without incorporating resilience strategy.

The system reserve states under the configuration that does not incorporate the resilient strategy are shown in Fig. 14, where 1 indicates that the configuration can meet the reserve requirement, while 0 indicates it cannot. In this situation, optimal planning considers only the operation economy, and the configuration adaptation to resilience requirements for supply-side outages is ignored. Therefore, a shortage of reserve will occur when facing heavy loads, i.e., critical loads will not be satisfied regardless of how much thermal energy is reserved. As shown in Fig. 14(a) of the cooling period, when the electricity supply failure occurs in the period of 23:00-0:00, 1:00-5:00 and 17:00-20:00, there will be curtailments for indispensable energy demands, and daily production and living conditions will be seriously affected.

But for the heating period, thermal storage reserve can be used to maintain enough operation resilience in the case of electrical/gas failure due to lower load level, even though the resilience is not considered in the planning process, as shown in Fig. 14(b). The reserve of thermal storage devices under the configuration without incorporating resilience strategy is presented in Fig. 15. In this scenario, the reserve is mainly used for the electricity outage when the loads are relatively higher. Restricted by the reserve constraints, the stored energy of hot-water tank at each time is larger than the required reserve capacity; thus, the necessary reserve is maintained and the supply-side outages can be well disposed by the application of the fault restoration strategy when executing the day-ahead scheduling.

2) ANALYSIS OF THE RESERVE STATE UNDER DIFFERENT CONFIGURATIONS

The scenarios of both cooling and heating periods with higher load levels (cooling period-Scenario 7, heating period-Scenario 1) are selected for the reserve analysis. The reserve states under the configuration incorporating the resilient strategy (i.e., whether the system can meet the reserve requirement in daily operation) are shown in Table 4 and Table 5. The system retains sufficient reserve capacity in the storage devices, and the critical loads can be fully satisfied by reasonable fault restoration strategy when supply-side outage occurs.

3) ANALYSIS OF THE FAULT RESTORATION UNDER DIFFERENT CONFIGURATIONS

In order to better highlight the advantages of the planning method considering the resilient strategy for dealing with supply-side outages in actual operation, Scenario 7 with a high load level in the cooling period is selected to analyse the fault restoration ability under two configurations.

Table 7 lists the fault restoration of two configurations in the case of electricity supply fault. It can be seen that the load restoration percentages are less than the percentages of the critical loads during the outage domain in some periods when the configuration is generated without the resilient strategy,

TABLE 7. Fault restoration for electricity outages.

Outage start period	Configuration without incorporating the resilient strategy				Configuration incorporating the resilient strategy			
	Satisfied load percentage (start interval)		Satisfied load percentage (next interval)		Satisfied load percentage (start interval)		Satisfied load percentage (next interval)	
	Electricity	Cooling	Electricity	Cooling	Electricity	Cooling	Electricity	Cooling
23	**0.616**	**1**	**0.548**	**1**	0.731	0.932	0.740	1
0	0.700	0.800	0.708	0.800	0.740	1	0.700	0.925
1	**0.701**	**0.997**	**0.465**	**1**	0.700	0.925	0.700	0.870
2	**0.663**	**1**	**0.477**	**1**	0.700	0.870	0.700	0.889
3	**0.662**	**1**	**0.487**	**1**	0.725	1	0.704	1
4	**0.476**	**1**	**0.717**	**1**	0.748	1	0.777	1
5	0.717	1	0.714	0.931	0.909	1	0.903	0.990
6	0.712	1	0.712	1	0.912	1	0.896	1
7	0.712	1	0.861	1	0.896	1	1	1
8	0.861	1	0.894	1	1	1	1	1
9	0.894	1	0.962	1	1	1	1	1
10	0.962	1	1	1	1	1	1	1
11	0.990	1	1	1	1	1	1	1
12	0.947	1	0.998	1	1	1	1	1
13	0.998	1	0.939	0.993	1	1	1	1
14	0.985	1	0.954	1	1	1	1	1
15	0.954	1	0.888	1	1	1	1	1
16	0.878	1	0.714	1	1	1	0.956	1
17	**0.756**	**1**	**0.618**	**1**	0.947	1	0.878	1
18	**0.684**	**1**	**0.583**	**1**	0.869	1	0.861	1
19	**0.670**	**1**	**0.576**	**1**	0.717	1	0.738	1
20	0.705	0.928	0.711	0.844	0.700	1	0.7	0.985
21	0.706	1	0.705	0.813	0.700	0.846	0.735	1
22	0.700	0.949	0.751	0.937	0.700	0.913	0.731	0.932

as shown in the bold font. After considering the resilient strategy in the planning process, the critical loads can be well satisfied due to the adaptability of the configuration to reserve requirements and the support of resilient scheduling strategy. The fault restoration scheme is optimized to minimize the objective function including the penalty cost of curtailed loads; thus, the satisfied proportion of the cooling load is larger than that of the electricity load owing to their different penalty costs.

Incorporating the results of the system configuration and reserve state, it is obvious that the proposed planning method fully considers the daily resilience demands for supply-side outages and can maintain sufficient reserves. And the supply of critical loads in outage domain can be guaranteed through the fault restoration means. At the same time, the overall annual cost after considering operation resilience increases slightly, the resilience and reliability are improved significantly with little sacrifice to the economy.

VI. CONCLUSION

This paper presents a two-level planning approach for integrated electricity and gas community energy system that considers the resilient scheduling strategy to determine the optimal configuration along with the operation. On the basis of modelling electricity and gas-driven devices and analysing the reserve modes, a multi-stage resilient scheduling strategy is first proposed for enhancing resilience, and the optimal planning method that takes into account the resilient scheduling is then established to improve the adaptation to the resilient requirements in actual operation. The operation data of a community energy system with practical demands are chosen to conduct a case study.

The proposed resilient strategy can fully utilize the complementary characteristics of gas/electricity subsystems and the auxiliary response features of storage devices to promote the resilience. After the storage reserve calculation in the rolling stage, multiple supply and storage devices are well

coordinated in the day-ahead stage to improve the economic performance, maintaining adequate reserves to cope with electricity and gas outages. In case that source supply breaks down, the critical loads can be well satisfied by the application of the fault restoration strategy.

In addition, the two-level planning method considering resilient scheduling can generate a more reasonable configuration for operation resilience against contingencies. Through the interaction of the configuration optimization level using the genetic algorithm and the operation optimization level by adopting the resilient scheduling strategy, the configuration which has stronger adaptability to the resilience requirements in actual operation can be obtained. The overall annual cost increases slightly compared with the configuration without considering resilience, achieving a better fault restoration effect by little sacrifice to the economy.

In conclusion, the optimal design and operation method with the support of multi-stage resilient strategy can effectively enhance the system resilience, guaranteeing sufficient reserve capacity in actual operation and realizing better fault restoration for supply-side outages.

To balance the optimality and efficiency for different scale systems, more efficient solution algorithms for large-scale mixed-integer programming should be developed in future work. For example, Benders-decomposition based method can be considered to lift the computational performance by separating integer variables and continuous variables.

APPENDIX

A. MODELLING OF ELECTRICITY-DRIVEN DEVICES

1) GROUND SOURCE HEAT PUMP

Ground source heat pump is a renewable energy technology for space cooling and space heating in different periods by using the ground as a heat/cooling source. During the cooling season, heat pump can be operated in two modes: cooling mode and cooling-storage mode, and cold-water tank can be equipped to store cooling energy. Different from the cooling period, heat pump can be only used for space heating during heating period because the output water temperature cannot reach suitable standard for heating storage.

a: COOLING PERIOD

The constraints on the heat pumps' power in cooling season are shown in Eqs. (A.1)-(A.4). The lower and upper limits of cooling and cooling-storage powers are presented in Eqs (A.1) and (A.2), respectively. Eqs. (A.3) and (A.4) constrain the heat pump numbers in cooling and cooling-storage modes. The operation mode/on-off state of the chillers and pumps is 1 when it is in the execution/on state and 0 otherwise.

$$N_t^{\mathrm{HP,C}}\underline{Q}^{\mathrm{HP,C}} \le Q_t^{\mathrm{HP,C}} \le N_t^{\mathrm{HP,C}}\overline{Q}^{\mathrm{HP,C}} \tag{A.1}$$

$$N_t^{\mathrm{HP,S}}\underline{Q}^{\mathrm{HP,S}} \le Q_t^{\mathrm{HP,S}} \le N_t^{\mathrm{HP,S}}\overline{Q}^{\mathrm{HP,S}} \tag{A.2}$$

$$N_t^{\mathrm{HP,C}} \le U_t^{\mathrm{HP,C}} N^{\mathrm{HP}} \tag{A.3}$$

$$N_t^{\mathrm{HP,S}} \le U_t^{\mathrm{HP,S}} N^{\mathrm{HP}} \tag{A.4}$$

The cooling mode and cooling-storage mode of heat pumps can't operate simultaneously, as shown in Eq. (A.5). Eq. (A.6) shows the constraints of heat pump number in cooling-storage mode. $N^{\mathrm{CT,CWP}}$ is the number of chilled water pumps (CWPs) of cold-water tanks.

$$U_t^{\mathrm{HP,C}} + U_t^{\mathrm{HP,S}} \le 1 \tag{A.5}$$

$$N_t^{\mathrm{HP,S}} \le N^{\mathrm{CT,CWP}} \tag{A.6}$$

Eq. (A.7) depicts that the number of CWPs in cooling state should meet the cooling request of cold-water tanks. Eq. (A.8) describes the charging or discharging behaviors of cold-water tanks. The cooling energy stored in cold-water tanks should not exceed the limit, as restricted in Eq. (A.9). Where $\varepsilon^{\mathrm{WT}}$ is the heat loss rate of the water tank, and N^{CT} represents the number of cold-water tanks.

$$\sum\nolimits_{i=1}^{N^{\mathrm{CT,CWP}}} U_{t,i}^{\mathrm{CT,CWP}}\overline{Q}^{\mathrm{CT,CWP}} \ge Q_t^{\mathrm{CT}} \tag{A.7}$$

$$W_t^{\mathrm{CT}} = \left(1-\varepsilon^{\mathrm{WT}}\right) W_{t-1}^{\mathrm{CT}} + Q_t^{\mathrm{HP,S}}\Delta t - Q_t^{\mathrm{CT}}\Delta t \tag{A.8}$$

$$0 \le W_t^{\mathrm{CT}} \le N^{\mathrm{CT}}\overline{W}^{\mathrm{CT}} \tag{A.9}$$

The cooling state of CTs and the cooling-storage mode of HP are distinguished by Eq. (A.10). Similarly, Eq. (A.11) shows that the cooling state of CTs and the cooling mode of HP can't appear at a same time. The relationships between the cooling states of CT and its CWP are depicted in Eqs. (A.12) and (A.13).

$$U_t^{\mathrm{CT}} + U_t^{\mathrm{HP,S}} \le 1 \tag{A.10}$$

$$U_t^{\mathrm{CT}} + U_t^{\mathrm{HP,C}} \le 1 \tag{A.11}$$

$$U_t^{\mathrm{CT}} \le \sum\nolimits_{i=1}^{N^{\mathrm{CT,CWP}}} U_{t,i}^{\mathrm{CT,CWP}} \tag{A.12}$$

$$U_t^{\mathrm{CT}} \ge U_{t,i}^{\mathrm{CT,CWP}}, \quad \forall i \in \Omega_{\mathrm{CWP}}^{\mathrm{CT}} \tag{A.13}$$

The electric power consumption of HPs is described in Eq. (A.14), where $\mathrm{COP}^{\mathrm{HP,C}}$ is the coefficient of performance (COP) of HP for cooling and cooling-storage; $P^{\mathrm{HP,C,AU}}$ and $P^{\mathrm{HP,S,AU}}$ are the rated powers of auxiliary equipment in cooling and cooling-storage mode, respectively.

$$P_t^{\mathrm{HP}} = \left(Q_t^{\mathrm{HP,C}} + Q_t^{\mathrm{HP,S}}\right) \Big/ \mathrm{COP}^{\mathrm{HP,C}} + N_t^{\mathrm{HP,C}} P^{\mathrm{HP,C,AU}} + N_t^{\mathrm{HP,S}} P^{\mathrm{HP,S,AU}} \tag{A.14}$$

The electric power consumption of cold-water tanks mainly lies in the circulating pumps installed on both sides of heat exchanger, which is given in Eq. (A.15). $P^{\mathrm{CT,AU}}$ is the rated power of auxiliary circulating pumps.

$$P_t^{\mathrm{CT}} = \sum\nolimits_{i=1}^{N^{\mathrm{CT,CWP}}} U_{t,i}^{\mathrm{CT,CWP}} P^{\mathrm{CT,AU}} \tag{A.15}$$

b: HEATING PERIOD

Similar to the cooling period, the constraints of ground source heat pumps in heating season are shown in Eqs. (A.16)-(A.18). Eq. (A.16) presents the power limits and Eq. (A.17) restrains the operating number in the heating mode. The consumed electric power of HPs is calculated by Eq. (A.18).

Where $\mathrm{COP}^{\mathrm{HP,H}}$ is the COP of HP for heating and $P^{\mathrm{HP,H,AU}}$ is the rated power of the auxiliary equipment in heating mode.

$$N_t^{\mathrm{HP,H}}\underline{Q}^{\mathrm{HP,H}} \le Q_t^{\mathrm{HP,H}} \le N_t^{\mathrm{HP,H}}\overline{Q}^{\mathrm{HP,H}} \tag{A.16}$$

$$N_t^{\mathrm{HP,H}} \le U_t^{\mathrm{HP,H}} N^{\mathrm{HP}} \tag{A.17}$$

$$P_t^{\mathrm{HP}} = Q_t^{\mathrm{HP,H}} \Big/ \mathrm{COP}^{\mathrm{HP,H}} + U_t^{\mathrm{HP,H}} N_t^{\mathrm{HP,H}} P^{\mathrm{HP,H,AU}} \tag{A.18}$$

2) CONVENTIONAL WATER-COOLED CHILLER

Eq. (A.19) restrains the maximum and minimum cooling powers of conventional water-cooled chillers. And the operating number of the units is limited by Eq. (A.20).

$$N_t^{\mathrm{WC}}\underline{Q}^{\mathrm{WC}} \le Q_t^{\mathrm{WC}} \le N_t^{\mathrm{WC}}\overline{Q}^{\mathrm{WC}} \tag{A.19}$$

$$N_t^{\mathrm{WC}} \le N^{\mathrm{WC}} \tag{A.20}$$

Eq. (A.21) describes the electric power consumption of WCs, where $\mathrm{COP}^{\mathrm{WC}}$ is the COP of WC and $P^{\mathrm{WC,AU}}$ is the rated power of interlocked auxiliary equipment.

$$P_t^{\mathrm{WC}} = Q_t^{\mathrm{WC}} \Big/ \mathrm{COP}^{\mathrm{WC}} + N_t^{\mathrm{WC}} P^{\mathrm{HP,H,AU}} \tag{A.21}$$

3) ICE-STORAGE SYSTEM

The ice-storage system contains several double-duty chillers and one ice-storage tank. In addition, double-duty chiller can operate in two modes, namely cooling mode and ice-making mode [12]. The cooling power can be provided by double-duty chillers and ice-storage tank, which is depicted in Eq. (A.22).

$$Q_t^{\mathrm{DC,C}} + Q_t^{\mathrm{IT}} = Q_t^{\mathrm{IS}} \tag{A.22}$$

The cooling/ice-making power of double-duty chillers is restrained within their allowed bounds by Eqs. (A.23) and (A.24). The number of the units in cooling and ice-making modes is also limited, as shown in Eqs. (A.25) and (A.26). Eq. (A.27) depicts that the two modes of double-duty chillers can't work in parallel.

$$N_t^{\mathrm{DC,C}}\underline{Q}^{\mathrm{DC,C}} \le Q_t^{\mathrm{DC,C}} \le N_t^{\mathrm{DC,C}}\overline{Q}^{\mathrm{DC,C}} \tag{A.23}$$

$$N_t^{\mathrm{DC,I}}\underline{Q}^{\mathrm{DC,I}} \le Q_t^{\mathrm{DC,I}} \le N_t^{\mathrm{DC,I}}\overline{Q}^{\mathrm{DC,I}} \tag{A.24}$$

$$N_t^{\mathrm{DC,C}} \le U_t^{\mathrm{DC,C}} N^{\mathrm{DC}} \tag{A.25}$$

$$N_t^{\mathrm{DC,I}} \le U_t^{\mathrm{DC,I}} N^{\mathrm{DC}} \tag{A.26}$$

$$U_t^{\mathrm{DC,C}} + U_t^{\mathrm{DC,I}} \le 1 \tag{A.27}$$

Eqs. (A.28) and (A.29) describe the charging or discharging behaviors of ice-storage tank and the stored energy limit, where $\varepsilon^{\mathrm{IT}}$ is the heat loss rate of ice-storage tank. The cooling power is restricted within the upper bound and is zero if double-duty chillers are charging to the ice-storage tank, which is shown in Eq. (A.30).

$$W_t^{\mathrm{IT}} = \left(1-\varepsilon^{\mathrm{IT}}\right) W_{t-1}^{\mathrm{IT}} + Q_t^{\mathrm{DC,I}}\Delta t - Q_t^{\mathrm{IT}}\Delta t \tag{A.28}$$

$$0 \le W_t^{\mathrm{IT}} \le M^{\mathrm{IT}} \tag{A.29}$$

$$0 \le Q_t^{\mathrm{IT}} \le \left(1-U_t^{\mathrm{DC,I}}\right)\overline{Q}^{\mathrm{IT}} \tag{A.30}$$

The operating number constraints of CWPs in the ice-storage system are described in Eqs. (A.31) and (A.32) according to "one chiller one pump" and the cooling requirements of the system.

$$\sum\nolimits_{i=1}^{N^{\mathrm{IS,CWP}}} U_{t,i}^{\mathrm{IS,CWP}} \ge N_t^{\mathrm{DC,C}} \tag{A.31}$$

$$\sum\nolimits_{i=1}^{N^{\mathrm{IS,CWP}}} U_{t,i}^{\mathrm{IS,CWP}}\overline{Q}^{\mathrm{IS,CWP}} \ge Q_t^{\mathrm{IS}} \tag{A.32}$$

The consumed electric power of ice-storage system can be calculated by Eq. (A.33), where $\mathrm{COP}^{\mathrm{DC,C}}$ and $\mathrm{COP}^{\mathrm{DC,I}}$ denote the COP of double-duty chiller in cooling mode and ice-making mode, respectively; $P^{\mathrm{DC,C,AU}}$ and $P^{\mathrm{DC,I,AU}}$ refer to the rated powers of auxiliary equipment in cooling mode and ice-making mode; P^{EP} and $P^{\mathrm{IS,CWP}}$ are the rated powers of ethylene glycol pump (EP) and CWP in ice-storage system, respectively.

$$\begin{aligned} P_t^{\mathrm{IS}} = {} & Q_t^{\mathrm{DC,C}}/\mathrm{COP}^{\mathrm{DC,C}} + Q_t^{\mathrm{DC,I}}/\mathrm{COP}^{\mathrm{DC,I}} + N_t^{\mathrm{DC,C}} P^{\mathrm{DC,C,AU}} \\ & + N_t^{\mathrm{DC,I}} P^{\mathrm{DC,I,AU}} + Q_t^{\mathrm{IS}} P^{\mathrm{EP}}/\overline{Q}^{\mathrm{EP}} \\ & + \sum\nolimits_{i=1}^{N^{\mathrm{IS,CWP}}} U_{t,i}^{\mathrm{IS,CWP}} P^{\mathrm{IS,CWP}} \end{aligned} \tag{A.33}$$

4) ELECTRIC BOILER SYSTEM WITH ACCUMULATOR

The heating power of electric boiler system with accumulator is the sum of heating power of electric boilers and hot-water tanks, as shown in Eq. (A.34). The heating power of electric boilers can be used for spacing heating and heating storage, as indicated in Eq. (A.35). Eq. (A.36) restricts the output power of electric boilers to be less than its limit, and Eq. (A.37) describes the operating number limit of electric boilers. The electric boilers and hot-water tanks can't work simultaneously, as shown in Eq. (A.38). Eq. (A.39) presents the electric power consumption of electric boilers. Where $Q_t^{\mathrm{EB,WT,H}}$ is the heating power of electric boiler system with accumulator; η^{EB} is the efficiency of electric boiler; $P^{\mathrm{EB,WP}}$ is the rated power of auxiliary circulating water pump.

$$Q_t^{\mathrm{EB,WT,H}} = Q_t^{\mathrm{EB,H}} + Q_t^{\mathrm{HT}} \tag{A.34}$$

$$Q_t^{\mathrm{EB}} = Q_t^{\mathrm{EB,H}} + Q_t^{\mathrm{EB,S}} \tag{A.35}$$

$$0 \le Q_t^{\mathrm{EB}} \le N_t^{\mathrm{EB}}\overline{Q}^{\mathrm{EB}} \tag{A.36}$$

$$N_t^{\mathrm{EB}} \le U_t^{\mathrm{EB}} N^{\mathrm{EB}} \tag{A.37}$$

$$U_t^{\mathrm{EB}} + U_t^{\mathrm{HT}} \le 1 \tag{A.38}$$

$$P_t^{\mathrm{EB}} = Q_t^{\mathrm{EB}} \Big/ \eta^{\mathrm{EB}} + N_t^{\mathrm{EB}} P^{\mathrm{EB,WP}} \tag{A.39}$$

The constraints of hot-water tanks are shown in Eqs. (A.40)-(A.42). Eq. (A.40) describes the relationship between the total stored heating energy and the charge/discharge power. Eqs. (A.41) and (A.42) restrict the heating energy stored in hot-water tanks and the heating power, respectively. N^{HT} represents the number of hot-water tanks. At the same time, the interlocked water pumps (i.e., circulation water pumps and supply water pumps) on both sides of the plate

heat exchanger should meet the heating requirement of electric boiler system and they will consume electric power, which can be seen in Eqs. (A.43) and (A.44), where $P^{\mathrm{HWP,C}}$ and $P^{\mathrm{HWP,S}}$ are the rated powers of circulation water pump and supply water pump, respectively.

$$W_t^{\mathrm{HT}} = \left(1-\varepsilon^{\mathrm{WT}}\right) W_{t-1}^{\mathrm{HT}} + Q_t^{\mathrm{EB,S}}\Delta t - Q_t^{\mathrm{HT}}\Delta t \tag{A.40}$$

$$0 \le W_t^{\mathrm{HT}} \le N^{\mathrm{HT}}\overline{W}^{\mathrm{HT}} \tag{A.41}$$

$$0 \le Q_t^{\mathrm{HT}} \le U_t^{\mathrm{HT}} N^{\mathrm{HT}}\overline{Q}^{\mathrm{HT}} \tag{A.42}$$

$$\sum\nolimits_{i=1}^{N^{\mathrm{HWP}}} U_{t,i}^{\mathrm{HWP}}\overline{Q}^{\mathrm{HWP}} \ge Q_t^{\mathrm{EB,H}} + Q_t^{\mathrm{HT}} \tag{A.43}$$

$$P_t^{\mathrm{HWP}} = \sum\nolimits_{i=1}^{N^{\mathrm{HWP}}} U_{t,i}^{\mathrm{HWP}}\left(P^{\mathrm{HWP,C}} + P^{\mathrm{HWP,S}}\right) \tag{A.44}$$

B. MODELLING OF GAS-DRIVEN DEVICES

1) GAS TURBINE

Gas turbine burns natural gas for power generation, and the heat can be recovered by waste heat recovery device for space heating and space cooling. This paper ignores the loss of heat recovery device, and the relationship between electric power P_t^{GT}, heating power H_t^{GT}, and gas consumption power F_t^{GT} are shown in Eqs. (A.45) and (A.46) [41]. And the constraints of output power and the operating number are presented in Eqs. (A.47) and (A.48).

$$P_t^{\mathrm{GT}} = \eta^{\mathrm{GT}} F_t^{\mathrm{GT}} \tag{A.45}$$

$$H_t^{\mathrm{GT}} = \alpha^{\mathrm{GT}} P_t^{\mathrm{GT}} \tag{A.46}$$

$$0 \le P_t^{\mathrm{GT}} \le N_t^{\mathrm{GT}}\overline{P}^{\mathrm{GT}} \tag{A.47}$$

$$N_t^{\mathrm{GT}} \le N^{\mathrm{GT}} \tag{A.48}$$

where η^{GT} and α^{GT} are the power generation efficiency and heat-electricity ratio of gas turbine, respectively.

2) ABSORPTION CHILLER

Absorption chiller can convert heating to cooling, and the relationship between consumed heating power Q_t^{AC} and output cooling power H_t^{AC} can be expressed by Eq. (A.49). The absorbed heating power is less than the heating output of gas turbine, as shown in Eq. (A.50). The cooling power and the operating number of absorption chillers can't exceed the limit and installed number, which are depicted in Eq. (A.51) and Eq. (A.52), respectively. $\mathrm{COP}^{\mathrm{AC}}$ is the COP of absorption chiller. Similarly, the consumed energy of auxiliary devices is ignored in this model due to its very little power consumption.

$$Q_t^{\mathrm{AC}} = \mathrm{COP}^{\mathrm{AC}} H_t^{\mathrm{AC}} \tag{A.49}$$

$$H_t^{\mathrm{AC}} \le H_t^{\mathrm{GT}} \tag{A.50}$$

$$0 \le Q_t^{\mathrm{AC}} \le N_t^{\mathrm{AC}}\overline{Q}^{\mathrm{AC}} \tag{A.51}$$

$$N_t^{\mathrm{AC}} \le N^{\mathrm{AC}} \tag{A.52}$$

C. MODELLING OF PHOTOVOLTAIC SYSTEM

Regardless of the temperature influence, PV system is assumed to produce electricity in proportion to solar radiation, as illustrated in Eq. (A.53). An additional constraint is essential to prevent the area of installed PV cells exceeding the roof area, as described in Eq. (A.54).

$$P_t^{\mathrm{PV}} = \frac{I_t}{I_{\mathrm{STC}}} M^{\mathrm{PV}} \tag{A.53}$$

$$M^{\mathrm{PV}} \le \overline{M}^{\mathrm{PV}} \tag{A.54}$$

where I_t is the solar radiation under actual operation; I_{STC} is the solar radiation under standard test condition; and $\overline{M}^{\mathrm{PV}}$ is the maximum installed capacity of PV system.

D. POWER BALANCE

The balance constraints of heating and cooling of the IEGS are shown in Eq. (A.55) and Eq. (A.56) respectively, and the electricity balance is described in Eq. (A.57). The purchasing powers of electricity and gas power should not exceed the maximum powers (see Eqs. (A.58) and (A.59)).

$$Q_t^{\mathrm{HP,H}} + Q_t^{\mathrm{EB,H}} + Q_t^{\mathrm{HT}} + H^{\mathrm{GT}} = L_t^{\mathrm{H}} \tag{A.55}$$

$$Q_t^{\mathrm{HP,C}} + Q_t^{\mathrm{CT}} + Q_t^{\mathrm{WC}} + Q_t^{\mathrm{IS}} + Q_t^{\mathrm{AC}} = L_t^{\mathrm{C}}$$

$$P_t^{\mathrm{TL}} + P_t^{\mathrm{PV}} + P_t^{\mathrm{GT}} = L_t^{\mathrm{E}} + P_t^{\mathrm{HP}} + P_t^{\mathrm{CT}} + P_t^{\mathrm{WC}} + P_t^{\mathrm{IS}} + P_t^{\mathrm{EB}} + P_t^{\mathrm{HWP}} \tag{A.56}$$

$$P_t^{\mathrm{TL}} \le P^{\mathrm{TL,max}} \tag{A.57}$$

$$F_t^{\mathrm{GT}} \le F^{\mathrm{GT,max}} \tag{A.58}$$

REFERENCES

[1] S. M. Ali, Z. Ullah, G. Mokryani, B. Khan, I. Hussain, C. A. Mehmood, U. Farid, and M. Jawad, "Smart grid and energy district mutual interactions with demand response programs," *IET Energy Syst. Integr.*, vol. 2, no. 1, pp. 1–8, Mar. 2020.

[2] H. Ameli, M. Qadrdan, and G. Strbac, "Coordinated operation strategies for natural gas and power systems in presence of gas-related flexibilities," *IET Energy Syst. Integr.*, vol. 1, no. 1, pp. 3–13, Mar. 2019.

[3] B. P. Koirala, E. Koliou, J. Friege, R. A. Hakvoort, and P. M. Herder, "Energetic communities for community energy: A review of key issues and trends shaping integrated community energy systems," *Renew. Sustain. Energy Rev.*, vol. 56, pp. 722–744, Apr. 2016.

[4] C. Wang, S. Dong, S. Xu, M. Yang, S. He, X. Dong, and J. Liang, "Impact of power-to-gas cost characteristics on power-gas-heating integrated system scheduling," *IEEE Access*, vol. 7, pp. 17654–17662, 2019.

[5] G. Li, R. Zhang, T. Jiang, H. Chen, L. Bai, H. Cui, and X. Li, "Optimal dispatch strategy for integrated energy systems with CCHP and wind power," *Appl. Energy*, vol. 192, pp. 408–419, Apr. 2017.

[6] J. Chen, W. Zhang, Y. Zhang, and G. Bao, "Day-ahead scheduling of distribution level integrated electricity and natural gas system based on fast-ADMM with restart algorithm," *IEEE Access*, vol. 6, pp. 17557–17569, 2018.

[7] I. G. Moghaddam, M. Saniei, and E. Mashhour, "A comprehensive model for self-scheduling an energy hub to supply cooling, heating and electrical demands of a building," *Energy*, vol. 94, pp. 157–170, Jan. 2016.

[8] W. Lin, X. Jin, Y. Mu, H. Jia, X. Xu, X. Yu, and B. Zhao, "A two-stage multi-objective scheduling method for integrated community energy system," *Appl. Energy*, vol. 216, pp. 428–441, Apr. 2018.

[9] R. Zhang, T. Jiang, G. Li, H. Chen, X. Li, L. Bai, and H. Cui, "Day-ahead scheduling of multi-carrier energy systems with multi-type energy storages and wind power," *CSEE J. Power Energy Syst.*, vol. 4, no. 3, pp. 283–292, Sep. 2018.

[10] Y. Wen, X. Qu, W. Li, X. Liu, and X. Ye, "Synergistic operation of electricity and natural gas networks via ADMM," *IEEE Trans. Smart Grid*, vol. 9, no. 5, pp. 4555–4565, Sep. 2018.

[11] M. Majidi, B. Mohammadi-Ivatloo, and A. Anvari-Moghaddam, "Optimal robust operation of combined heat and power systems with demand response programs," *Appl. Thermal Eng.*, vol. 149, pp. 1359–1369, Feb. 2019.

[12] Y. Ruan, Q. Liu, Z. Li, and J. Wu, "Optimization and analysis of building combined cooling, heating and power (BCHP) plants with chilled ice thermal storage system," *Appl. Energy*, vol. 179, pp. 738–754, Oct. 2016.
[13] Z. Liu, H. Yu, and R. Liu, "A novel energy supply and demand matching model in park integrated energy system," *Energy*, vol. 176, pp. 1007–1019, Jun. 2019.
[14] Q. Zeng, B. Zhang, J. Fang, and Z. Chen, "A bi-level programming for multistage co-expansion planning of the integrated gas and electricity system," *Appl. Energy*, vol. 200, pp. 192–203, Aug. 2017.
[15] V. Khaligh and A. Anvari-Moghaddam, "Stochastic expansion planning of gas and electricity networks: A decentralized-based approach," *Energy*, vol. 186, Nov. 2019, Art. no. 115889.
[16] V. Khaligh, M. Oloomi Buygi, A. Anvari-Moghaddam, and J. M. Guerrero, "A multi-attribute expansion planning model for integrated gas–electricity system," *Energies*, vol. 11, no. 10, p. 2573, 2018.
[17] A. Alabdulwahab, A. Abusorrah, X. Zhang, and M. Shahidehpour, "Coordination of interdependent natural gas and electricity infrastructures for firming the variability of wind energy in stochastic day-ahead scheduling," *IEEE Trans. Sustain. Energy*, vol. 6, no. 2, pp. 606–615, Apr. 2015.
[18] T. Li, M. Eremia, and M. Shahidehpour, "Interdependency of natural gas network and power system security," *IEEE Trans. Power Syst.*, vol. 23, no. 4, pp. 1817–1824, Nov. 2008.
[19] Y. Lei, K. Hou, Y. Wang, H. Jia, P. Zhang, Y. Mu, X. Jin, and B. Sui, "A new reliability assessment approach for integrated energy systems: Using hierarchical decoupling optimization framework and impact-increment based state enumeration method," *Appl. Energy*, vol. 210, pp. 1237–1250, Jan. 2018.
[20] G. Li, R. Zhang, T. Jiang, H. Chen, L. Bai, and X. Li, "Security-constrained bi-level economic dispatch model for integrated natural gas and electricity systems considering wind power and power-to-gas process," *Appl. Energy*, vol. 194, pp. 696–704, May 2017.
[21] Y. Wang, C. Chen, J. Wang, and R. Baldick, "Research on resilience of power systems under natural disasters—A review," *IEEE Trans. Power Syst.*, vol. 31, no. 2, pp. 1604–1613, Mar. 2016.
[22] M. Panteli, D. N. Trakas, P. Mancarella, and N. D. Hatziargyriou, "Boosting the power grid resilience to extreme weather events using defensive islanding," *IEEE Trans. Smart Grid*, vol. 7, no. 6, pp. 2913–2922, Nov. 2016.
[23] H. Gao, Y. Chen, Y. Xu, and C.-C. Liu, "Resilience-oriented critical load restoration using microgrids in distribution systems," *IEEE Trans. Smart Grid*, vol. 7, no. 6, pp. 2837–2848, Nov. 2016.
[24] J. Najafi, A. Peiravi, A. Anvari-Moghaddam, and J. M. Guerrero, "An efficient interactive framework for improving resilience of power-water distribution systems with multiple privately-owned microgrids," *Int. J. Elect. Power Energy Syst.*, vol. 116, Mar. 2020, Art. no. 105550.
[25] X. Zhang, M. Shahidehpour, A. Alabdulwahab, and A. Abusorrah, "Hourly electricity demand response in the stochastic day-ahead scheduling of coordinated electricity and natural gas networks," *IEEE Trans. Power Syst.*, vol. 31, no. 1, pp. 592–601, Jan. 2016.
[26] C. Wang, W. Wei, J. Wang, F. Liu, F. Qiu, C. M. Correa-Posada, and S. Mei, "Robust defense strategy for gas–electric systems against malicious attacks," *IEEE Trans. Power Syst.*, vol. 32, no. 4, pp. 2953–2965, Jul. 2017.
[27] M. Yan, Y. He, M. Shahidehpour, X. Ai, Z. Li, and J. Wen, "Coordinated regional-district operation of integrated energy systems for resilience enhancement in natural disasters," *IEEE Trans. Smart Grid*, vol. 10, no. 5, pp. 4881–4892, Sep. 2019.
[28] C. Shao, M. Shahidehpour, X. Wang, X. Wang, and B. Wang, "Integrated planning of electricity and natural gas transportation systems for enhancing the power grid resilience," *IEEE Trans. Power Syst.*, vol. 32, no. 6, pp. 4418–4429, Nov. 2017.
[29] J. Najafi, A. Peiravi, A. Anvari-Moghaddam, and J. M. Guerrero, "Resilience improvement planning of power-water distribution systems with multiple microgrids against hurricanes using clean strategies," *J. Cleaner Prod.*, vol. 223, pp. 109–126, Jun. 2019.
[30] F. Wang and K. W. Hedman, "Dynamic reserve zones for day-ahead unit commitment with renewable resources," *IEEE Trans. Power Syst.*, vol. 30, no. 2, pp. 612–620, Mar. 2015.
[31] Y. Zhou, W. Hu, Y. Min, and Y. Dai, "Integrated power and heat dispatch considering available reserve of combined heat and power units," *IEEE Trans. Sustain. Energy*, vol. 10, no. 3, pp. 1300–1310, Jul. 2019.
[32] Y. He, M. Shahidehpour, Z. Li, C. Guo, and B. Zhu, "Robust constrained operation of integrated electricity-natural gas system considering distributed natural gas storage," *IEEE Trans. Sustain. Energy*, vol. 9, no. 3, pp. 1061–1071, Jul. 2018.
[33] F. Liu, Z. Bie, and X. Wang, "Day-ahead dispatch of integrated electricity and natural gas system considering reserve scheduling and renewable uncertainties," *IEEE Trans. Sustain. Energy*, vol. 10, no. 2, pp. 646–658, Apr. 2019.
[34] C. He, C. Dai, L. Wu, and T. Liu, "Robust network hardening strategy for enhancing resilience of integrated electricity and natural gas distribution systems against natural disasters," *IEEE Trans. Power Syst.*, vol. 33, no. 5, pp. 5787–5798, Sep. 2018.
[35] C. Wang, C. Lv, P. Li, G. Song, S. Li, X. Xu, and J. Wu, "Modeling and optimal operation of community integrated energy systems: A case study from China," *Appl. Energy*, vol. 230, pp. 1242–1254, Nov. 2018.
[36] J.-J. Wang, Y.-Y. Jing, and C.-F. Zhang, "Optimization of capacity and operation for CCHP system by genetic algorithm," *Appl. Energy*, vol. 87, no. 4, pp. 1325–1335, Apr. 2010.
[37] IBM Academic Initiative. *IBM ILOG CPLEX Optimization Studio*. Accessed: Oct. 11, 2019. [Online]. Available: https://www.ibm.com/products/Ilog-cplex-optimization-studio
[38] W. Huang, N. Zhang, J. Yang, Y. Wang, and C. Kang, "Optimal configuration planning of multi-energy systems considering distributed renewable energy," *IEEE Trans. Smart Grid*, vol. 10, no. 2, pp. 1452–1464, Mar. 2019.
[39] S. D. Manshadi and M. E. Khodayar, "Preventive reinforcement under uncertainty for islanded microgrids with electricity and natural gas networks," *J. Mod. Power Syst. Clean Energy*, vol. 6, no. 6, pp. 1223–1233, Nov. 2018.
[40] L. Li, H. Mu, W. Gao, and M. Li, "Optimization and analysis of CCHP system based on energy loads coupling of residential and office buildings," *Appl. Energy*, vol. 136, pp. 206–216, Dec. 2014.
[41] C. Wouters, E. S. Fraga, and A. M. James, "An energy integrated, multi-microgrid, MILP (mixed-integer linear programming) approach for residential distributed energy system planning—A south Australian case-study," *Energy*, vol. 85, pp. 30–44, Jun. 2015.

CHAOXIAN LV was born in Shangqiu, Henan, China, in 1989. He received the B.S. and M.S. degrees in electrical engineering from Hunan University, Changsha, China, in 2011 and 2014, respectively, and the Ph.D. degree in electrical engineering from Tianjin University, Tianjin, China, in 2019. He is currently a Lecturer with the School of Electrical and Power Engineering, China University of Mining and Technology. His current research interests include the operation, planning, and analysis of integrated energy system.

HAO YU (Member, IEEE) received the B.S. and Ph.D. degree in electrical engineering from Tianjin University, Tianjin, China, in 2010 and 2015, respectively. He is currently a Lecturer with the School of Electrical and Information Engineering, Tianjin University. His research interests include microgrids and active distribution systems.

PENG LI (Member, IEEE) received the B.S. and Ph.D. degrees in electrical engineering from Tianjin University, Tianjin, China, in 2004 and 2010, respectively. He is currently an Associate Professor with the School of Electrical and Information Engineering, Tianjin University. His current research interests include operation optimization of distribution networks and integrated energy systems, and analysis and transient simulation of power systems.

HAILONG LI received the Ph.D. degree from the Division of Energy Processes, Royal Institute of Technology (KTH), Sweden, in 2008. He is currently with the School of Business, Society and Engineering, Malardalen University, Sweden. His current research interests mainly include the mitigation of the climate change, and the efficient conversion and utilization of energy.

KUNPENG ZHAO was born in Handan, Hebei, China, in 1976. He is currently a Senior Engineer with the State Grid Customer Service Centre. His research fields include integrated energy service and smart scheduling of the energy Internet.

SHUQUAN LI was born in 1964. He is currently a Professorate Senior Engineer with the State Grid Customer Service Centre. His research fields include microgrids, energy internet, and smart energy system.